Bioorganic Chemistry 110 (2021) 104814

Contents lists available at ScienceDirect

Bioorganic Chemistry

journal homepage: www.elsevier.com/locate/bioorg

Synthesis and biological evaluation of disulfides as anticancer agents with thioredoxin inhibition

Xiangxu Wei [a], Miao Zhong [a], Song Wang [a], Lexun Li [a], Zi-Long Song [a], Junmin Zhang [a,b,*], Jianqiang Xu [c], Jianguo Fang [a,*]

[a] State Key Laboratory of Applied Organic Chemistry & College of Chemistry and Chemical Engineering, Lanzhou University, Lanzhou 730000, China
[b] School of Pharmacy, Lanzhou University, Lanzhou 730000, China
[c] School of Life and Pharmaceutical Sciences & Panjin Institute of Industrial Technology, Dalian University of Technology, Panjin 124221, China

ARTICLE INFO

Keywords:
Thioredoxin
Disulfide
Oxidative stress
Apoptosis
Anticancer

ABSTRACT

Altered redox homeostasis as a hallmark of cancer cells is exploited by cancer cells for growth and survival. The thioredoxin (Trx), an important regulator in maintaining the intracellular redox homeostasis, is cumulatively recognized as a promising target for the development of anticancer drugs. Herein, we synthesized 72 disulfides and evaluated their inhibition for Trx and antitumor activity. First, we established an efficient and fast method to screen Trx inhibitors by using the probe NBL-SS that was developed by our group to detect Trx function in living cells. After an initial screening of the Trx inhibitory activity of these compounds, 8 compounds showed significant inhibition activity against Trx. We then evaluated the cytotoxicity of these 8 disulfides, compounds **68** and **69** displayed high cytotoxicity to HeLa cells, but less sensitive to normal cell lines. Next, we performed kinetic studies of both two disulfides, **68** had faster inhibition of Trx than **69**. Further studies revealed that **68** led to the accumulation of reactive oxygen species and eventually induced apoptosis of Hela cells *via* inhibiting Trx. The establishment of a method for screening Trx inhibitors and the discovery of **68** with remarkable Trx inhibition provide support for the development of anticancer candidates with Trx inhibition.

1. Introduction

Cancer is still considered one of the most fatal diseases in the world [1]. Currently, chemotherapy is the most common and effective cancer therapy strategy, but the efficacy of chemotherapy is still limited due to the side effects of drugs and the increasing tolerance of treatment. The major problem now is the lack of effective anticancer medicines [2,3]. Therefore, it is imperative to discover highly effective lead molecules for anticancer drugs.

Thioredoxin (Trx), a ubiquitous redox regulator, is a key component of the intact thioredoxin system. Trx system and glutathione (GSH) system are predominant in regulating the intracellular redox homeostasis [4–6]. Several studies have shown that the function of Trx in cancer cells depends on the stage of cancer development [7–10]. In the early stage, Trx can resist the oxidative stress caused by carcinogens to prevent carcinogenesis. However, once the malignant phenotype has been established, the high concentration of Trx may accelerate the development of cancer cells, which promotes tumor growth and prevents cancer cell apoptosis [11]. Importantly, many primary tumor cell lines including cervical carcinomas [12], prostate cancer [13], breast cancer [14], colorectal cancer [15], pancreatic cancer [16], hepatocellular carcinoma [17], oral squamous cell carcinoma [18], gastric carcinoma [19], leukemia [20], and lung cancer [21] have high-level Trx. Researchers demonstrated that Trx overexpression could increase the production of vascular endothelial growth factors and promote tumor angiogenesis [22]. Trx is also implicated in highly invasive and metastatic tumor activity both *in vitro* and in vivo [23,24]. In addition, the resistance of tumor cells to various chemotherapy drugs is associated with high-level Trx [9,25]. Collectively, these studies suggest that Trx plays a positive functional role in promoting cancer cell growth. Thus,

Abbreviations: DCFH-DA, 2′, 7′-dichlorfluorescein diacetate; DCM, dichloromethane; DHE, dihydroethidium; DMSO, dimethyl sulfoxide; DTT, DL-dithiothreitol; GSH, glutathione; MTT, 3-(4, 5-Dimethylthiazol-2-yl)-2,5- diphenyltetrazolium bromid; PX-12, 2-[(1-Methylpropyl) dithio]-1H- imidazole; ROS, reactive oxygen species; SAR, structure-activity relationships; Trx, thioredoxin; TrxR, thioredoxin reductase.

* Corresponding authors at: State Key Laboratory of Applied Organic Chemistry & College of Chemistry and Chemical Engineering, Lanzhou University, Lanzhou 730000, China (J. Zhang).

E-mail addresses: zhangjunmin@lzu.edu.cn (J. Zhang), fangjg@lzu.edu.cn (J. Fang).

https://doi.org/10.1016/j.bioorg.2021.104814
Received 11 October 2020; Received in revised form 19 February 2021; Accepted 6 March 2021
Available online 10 March 2021

Trx may be regarded as a potential target in the development of anticancer drugs [26]. Once Trx is inhibited by small molecules, it will inevitably produce a large amount of reactive oxygen species (ROS), induce oxidative stress, and eventually promote cancer cell death [6,27,28].

Intriguingly, as far as the redox cycle of the entire Trx system is concerned, thioredoxin reductase (TrxR) takes electrons from NADPH and transfers them to Trx, Trx then directly interacts with various redox-active proteins through free thiol and disulfide exchange reactions [29,30]. Therefore, it is valuable to design and synthesize a series of small molecule disulfides to inhibit Trx through free thiol and disulfide exchange reactions. Existing structure-activity relationships (SAR) evidence suggests that half of the active molecule should be aromatic groups with electron-withdrawing substituents. It will bring substantial improvements in increasing activity [26,31]. An excellent example is PX-12 (2-[(1-Methylpropyl) dithio]-1H-imidazole), which has been clinically evaluated in cancer patients [32-34]. Khosla C. *et al.* developed another agent 2-(Cyclohexyldisulfanyl)-5- nitro-1H-benzo[*d*]imidazole, which could oxidize extracellular Trx *via* selective disulfide bond exchange [31]. It has been confirmed that these reported compounds primarily act on the conserved active site of Trx Cys32/Cys35, and also react slowly and irreversibly with the non-catalytic site Cys73 of Trx. [31,35-37].

To develop highly effective small molecule lead compounds as anticancer candidates with Trx inhibition, we established a molecular library with 72 disulfides. In recent years, researchers have developed many small molecular probes of protein thiols [38]. In view of this, we established an efficient and fast method to screen Trx inhibitors by using the probe NBL-SS developed by our group [39]. After an initial screening of all compounds, we evaluated the cytotoxicity of these disulfides and performed their kinetic studies. A preliminary description and summary of SAR are helpful to further optimize disulfides as anticancer candidates with Trx inhibition. Compound **68** displayed the greatest potency as an inhibitor for Trx among all compounds. Therefore, **68** was selected for the follow-up studies. Further research found that **68** might inhibit Trx by targeting the sulfhydryl groups, leading to the accumulation of ROS and promoting the apoptosis of tumor cells. We expect the lead compound **68** to be used as an anticancer candidate with Trx inhibition.

2. Results and discussion

2.1. Chemistry

In this study, all compounds were synthesized through the routes outlined in Scheme 1–3, and all of them were obtained through the corresponding thiols or thiophenols, respectively. Compounds **1**–**14** were synthesized according to the method described by Sun, L. *et al.* [40], compounds **15**–**53** were synthesized according to the method described by Stellenboom, N. *et al.* [41], compounds **54**–**72** were synthesized according to the method described by Khosla, C. *et al.* [31]. All compounds were characterized by ^{1}H NMR, ^{13}C NMR with a Bruker AMX spectrometer at 400 and 100 MHz, respectively. MS spectra were obtained using a Hewlett-Packard 5988A spectrometer or a Shimadzu LC-MS-2020 system.

2.2. Screening and SAR studies

As shown in Fig. 1, all compounds were screened by the small molecule probe NBL-SS [39]. The concentrations of compounds were 100 μM, 20 μM, and 10 μM, respectively. We set the fluorescence intensity at F_0 when the fluorescence of the probe was released fully. In the experiment, the fluorescence intensity was measured as F. When F/F_0 reached 100%, which indicated that the Trx was not inhibited by the compounds. As shown in Fig. 1 **A,** when the concentration of the compounds was 100 μM, most of the compounds were able to inhibit *E.coli* Trx and the fluorescence of the probe NBL-SS could not be released. To screen out more ideal compounds, the concentration of compounds was reduced to 20 μM to further narrow the range of compounds (Fig. 1 **B**). Finally, when the concentration of the compound was set to 10 μM, we found that compounds **4, 5, 6, 19, 22, 24, 68,** and **69** exhibit apparent oxidation capacity toward *E. coli* Trx **(**Fig. 1 **C).** Then, these 8 compounds and PX-12 were analyzed for cytotoxicity against HeLa, HepG2, BEAS-2B, and HEK-293T by using the MTT assay. Under this condition, the concentrations that inhibit the cell proliferation to 50% of the control (IC_{50} values) are summarized in Table 1. Compounds **68** and **69** displayed significant cytotoxicity toward HeLa cells and exhibited higher cytotoxicity than PX-12. In contrast, normal cell lines, including BEAS-2B and HEK-293T cells, were less sensitive to **68** and **69**. It shows that the compounds have great selectivity for tumor cell lines. Next, we chose these two compounds for further studies.

A preliminary SAR showed that the symmetric disulfides in the screened compounds have a good oxidation effect on protein, but they have low cytotoxicity to cancer cells and could not kill cancer cells well. In contrast, asymmetric disulfides not only have a good oxidation effect on protein, but also have high cytotoxicity. Especially when half of the molecule is aromatic groups with electron-withdrawing substituents, those compounds are worthy of further study. Intriguingly, we found that those molecules might also relieve the stench of the disulfide.

2.3. Oxidation capacity of compounds to Trx

Holmgren A. has proved that the fluorescence of *E. coli* Trx could decrease 2-fold when the reduced *E. coli* Trx is oxidized enzymatically or chemically [42]. Likewise, our results showed that when compound **68**

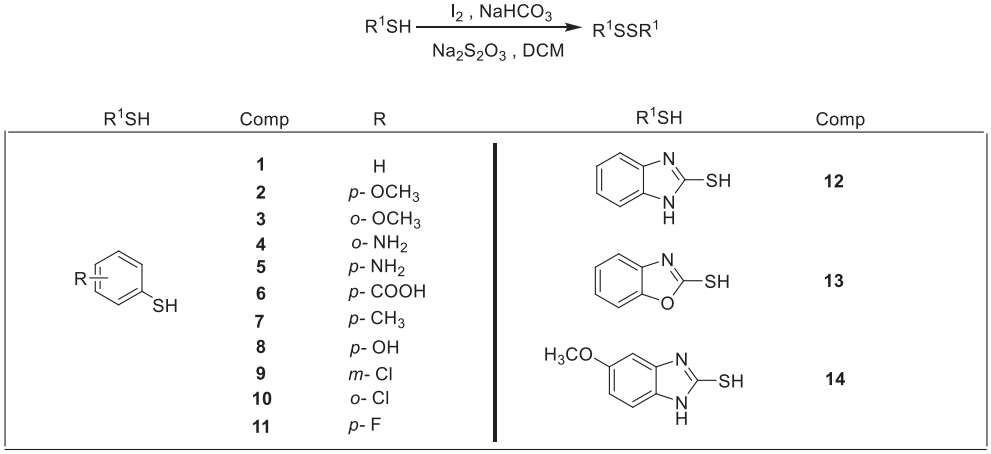

Scheme 1. General synthetic procedures for compounds **1**–**14**.

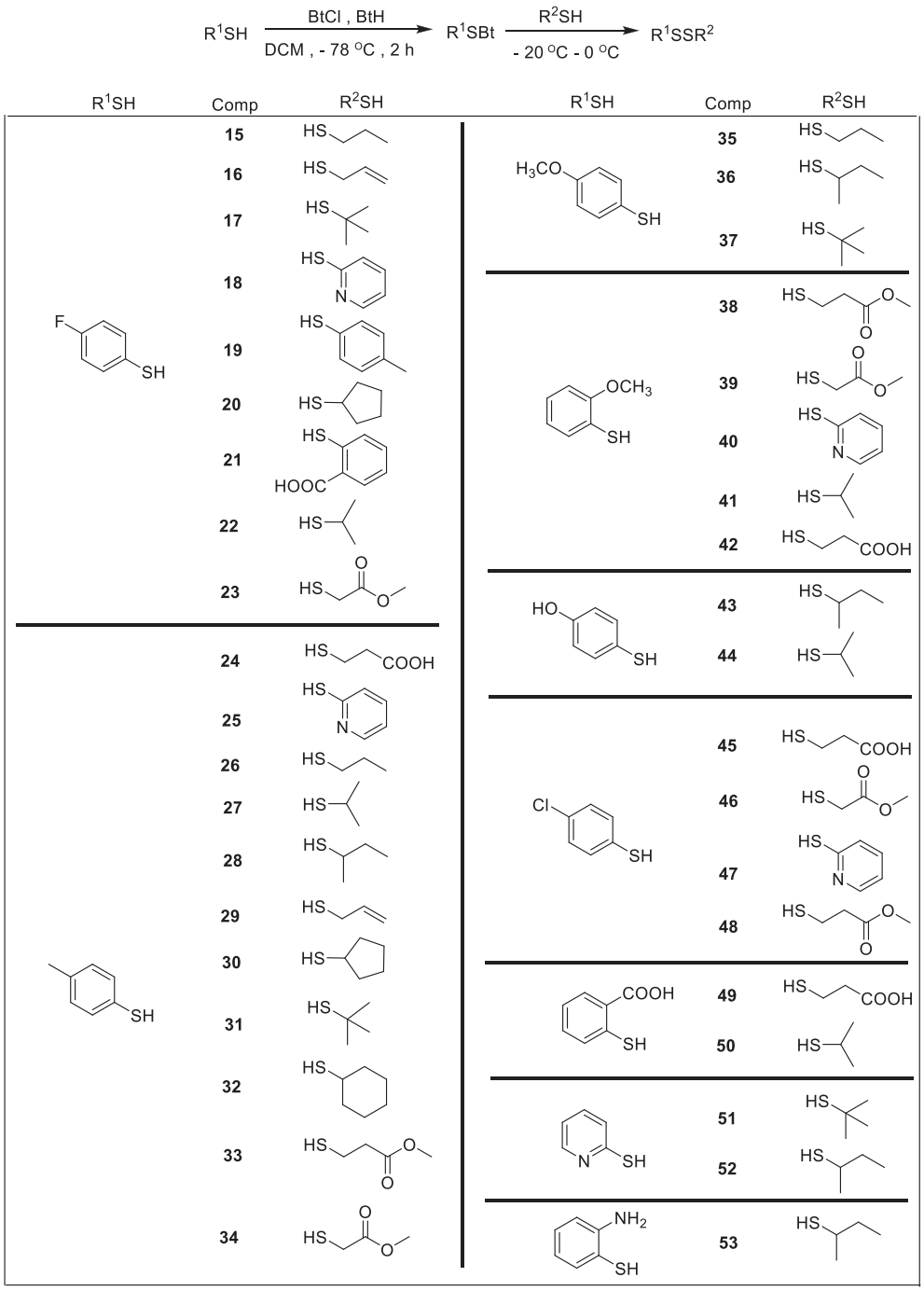

Scheme 2. General synthetic procedures for compounds **15**–**53**.

reacted with *E. coli* Trx, the fluorescence of Trx also could reduce 2-fold (**Fig. S1**). Then we determined the change of fluorescence intensity of *E. coli* Trx reacted with **68** and **69**, respectively. *E. coli* Trx was oxidized by **68** faster than it was oxidized by **69** (Fig. 2**A, B**). Therefore, we fitted the change of fluorescence intensity of *E. coli* Trx to the second-order rate equation for kinetic studies. Then, we determined the reaction rate constants of the compounds with *E. coli* Trx, and the second-order rate constants of **68** and **69** are 1290 $(M\ s)^{-1}$ and 910 $(M\ s)^{-1}$, respectively. The response between Trx and **68** was faster than **69**. The details of the calculation are shown in **Fig. S2** and **Tables S1-S2**. Next, we determined the optimal concentration and time of the reaction between **68** and Trx *via* the changes in fluorescence intensity of the redox state of *E.coli* Trx. As shown in Fig. 2**C**, the fluorescence intensity decreased with time-dependent and concentration-dependent, and the optimal concentration and time were also determined. After *E.coli* Trx was incubated with **68**, the redox state of *E.coli* Trx can be determined by probe Naph-EA-mal developed previously by our group [43]. Obviously, the fluorescence intensity decreased with time-dependent and concentration-dependent (Fig. 2**D, E**). Through the above experiments, we found that the reaction between Trx and 68 might be stoichiometric, and it was verified by HPLC (**Fig. S3**).

2.4. Cytotoxicity of compound *68*

Since compound **68** can oxidize Trx faster than **69**, we chose compound **68** for further studies. We measured the cytotoxicity of **68** by

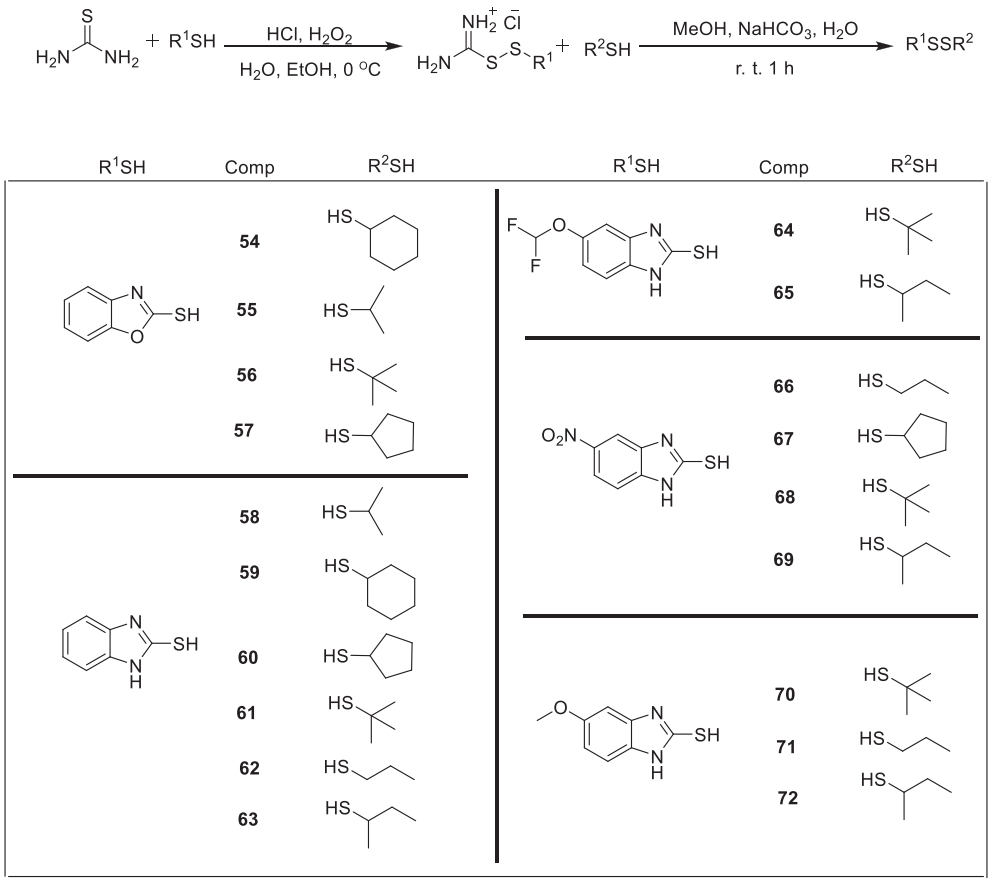

Scheme 3. General synthetic procedures for compounds **54**–**72**.

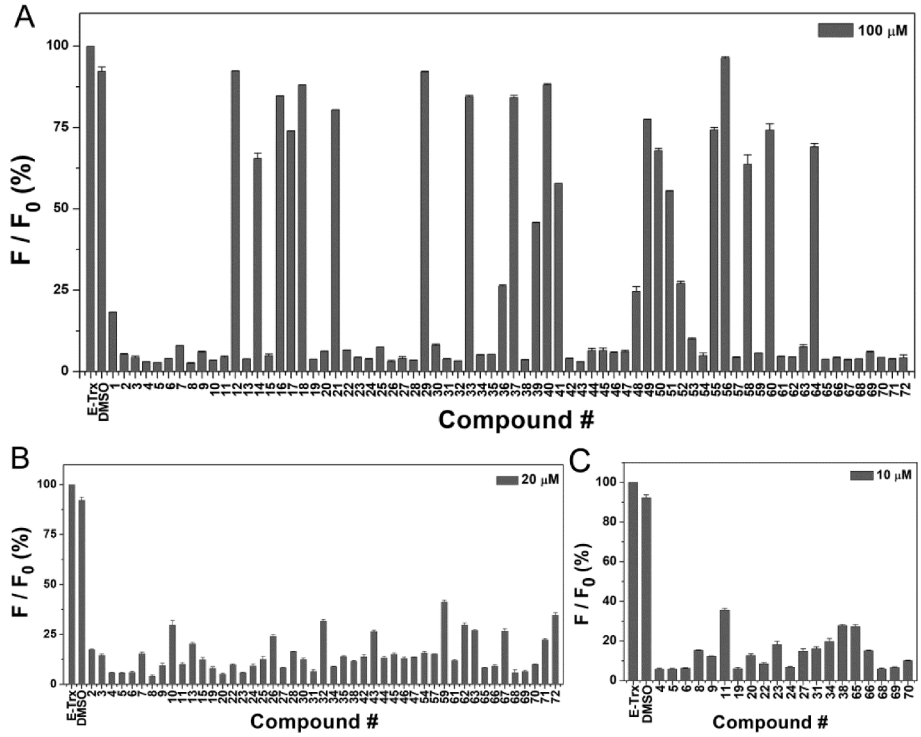

Fig. 1. Screening of disulfides against *E.coli* Trx with NBL-SS. Reduced Trx (10 μM) was incubated with different concentrations of compounds (A) 100 μM, (B) 20 μM, and (C) 10 μM at 37 °C in 96-well plates for 30 min. The E-Trx control group has reduced E-Trx and NBL-SS (5 μM), and the DMSO control has reduced E-Trx, DMSO and NBL-SS (5 μM). The probe NBL-SS was then added and incubated for 5 min, and the fluorescence intensity was monitored with a Microplate Reader (FlexStation 3, USA). Results are expressed as means ± SD of three independent experiments.

Table 1
Cytotoxicity of **4**, **5**, **6**, **19**, **22**, **24**, **68**, **69** and PX-12.

Compd.	IC_{50} (μM)[a]			
	HeLa	HepG2	HEK-293 T	BEAS-2B
4	24.5 ± 0.6	32.2 ± 2.5	44.3 ± 1.8	35.7 ± 0.3
5	19.1 ± 1.0	22.5 ± 2.1	22.7 ± 1.4	29.3 ± 1.4
6	17.1 ± 0.8	33.4 ± 0.9	33.8 ± 0.6	32.2 ± 2.8
19	16.5 ± 2.2	21.7 ± 2.1	22.2 ± 0.5	34.1 ± 2.2
22	16.6 ± 2.7	24.0 ± 1.6	19.5 ± 0.5	35.4 ± 2.9
24	15.3 ± 1.8	25.2 ± 2.1	22.9 ± 0.8	28.6 ± 2.2
68	9.3 ± 1.1	24.6 ± 2.0	33.3 ± 1.8	31.8 ± 2.6
69	12.3 ± 0.8	28.8 ± 1.3	29.0 ± 2.4	24.4 ± 0.9
PX-12	13.1 ± 1.6	29.0 ± 1.7	22.4 ± 0.9	38.0 ± 2.3

[a] The data were obtained by the MTT assay after a 72 h treatment.

MTT assay for different time (Fig. 3**A**). To confirm the results of the MTT assay, we further employed the trypan blue exclusion assay to assess cell viability. The results of the trypan blue exclusion assay and MTT assay are powerful consistent (Fig. 3**B**). In addition, the cytotoxicity of compound **68** showed a significant concentration and time dependence (**Fig. A & B**).

2.5. Imaging of Trx activity in live cells

The probe NBL-SS was designed in our lab could be applied to image Trx activity in live cells and in *vivo* conveniently [39]. HeLa cells were seeded in 12-well plates. After 24 h, the cells were treated with **68** (10 μM) for different time. Then NBL-SS (5 μM) was added and continued incubated for 5 min at 37 °C. The blank group was only incubated with **68** (10 μM) without the addition of the probe NBL-SS (5 μM). The cells were visualized and photographed under a fluorescent microscope. The appearance of red fluorescence indicated the activity of Trx in cells. As shown in Fig. 4**A**, we did not detect a bright red fluorescence signal in the blank group, while fluorescence in the cells treated by the **68** became weaker as time increased. In addition, we performed a quantitative analysis of fluorescence signal (Fig. 4**B**). The fluorescence intensity decreased with the incubation time. It proved that Trx could be inhibited effectively by compound **68** in the HeLa cells.

2.6. Alteration of Trx redox status

As mentioned above, **68** acted as an inhibitor of Trx. Therefore, detecting the redox status of Trx in cells could directly prove that Trx

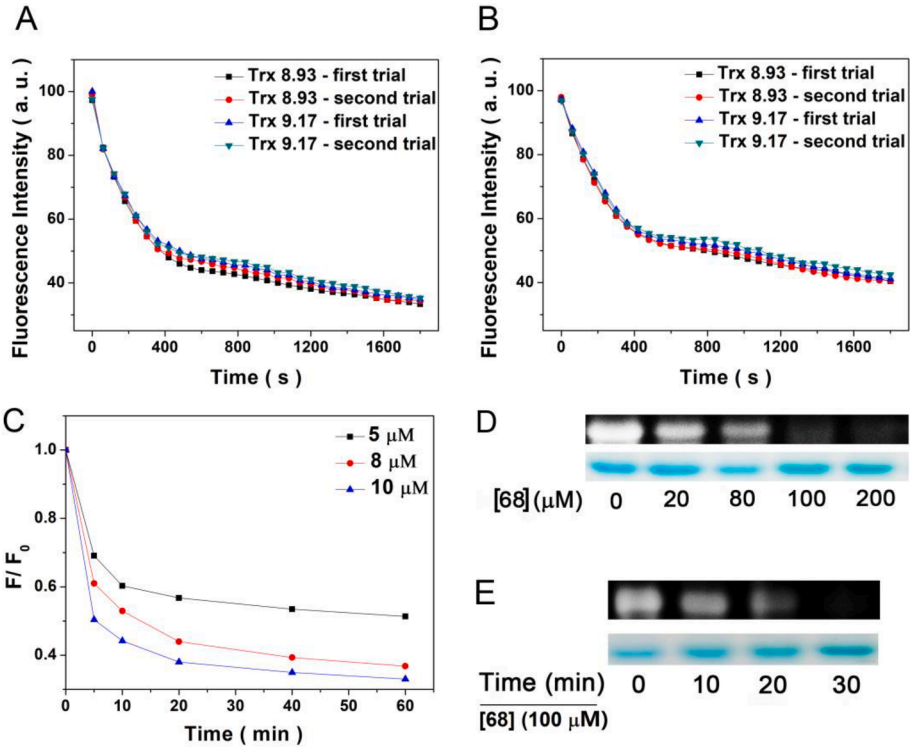

Fig. 2. Oxidation capacity of compounds to *E.coli* Trx. (A) Time-dependent fluorescence intensity change of Trx (8.93 μM and 9.17 μM, respectively) with **68** (10.0 μM). (B) Time-dependent fluorescence intensity change of Trx (8.93 μM and 9.17 μM, respectively) with **69** (10.0 μM). (C) Time- and dose-dependent fluorescence intensity change of **68** in response to Trx (10 μM). (D) The dose-dependent and (E) the time-dependent of **68** (100 μM) in response to Trx (100 μM), Trx redox states were determined by probe Naph-EA-mal and were separated by SDS-PAGE.

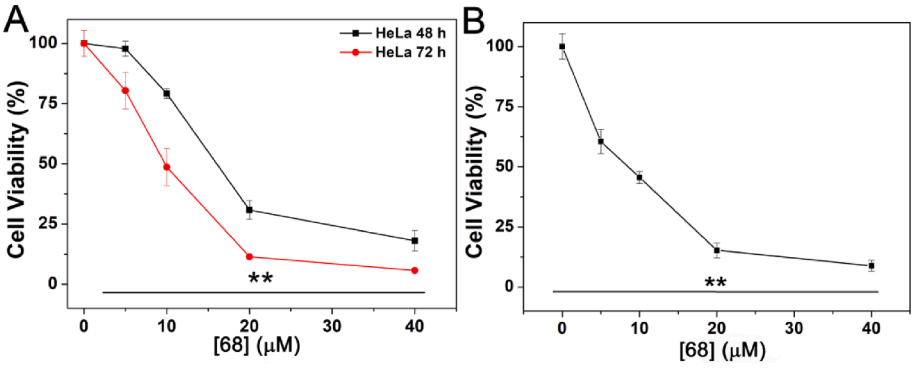

Fig. 3. Cytotoxicity of compound **68.** (A) Dose- and time-dependent cytotoxicity of **68** towards HeLa cells. The HeLa cells were incubated with varying concentrations of **68** for 48 h or 72 h. The cell viability was assessed by the MTT method. (B) Cytotoxicity of **68** towards HeLa cells for 72 h. The cell viability was determined by the trypan blue exclusion assay. Data are expressed as mean ± SE from triplicates. ** $P < 0.01$ vs. the control groups in (A) and (B). (For interpretation of the references to colour in this figure legend, the reader is referred to the web version of this article.)

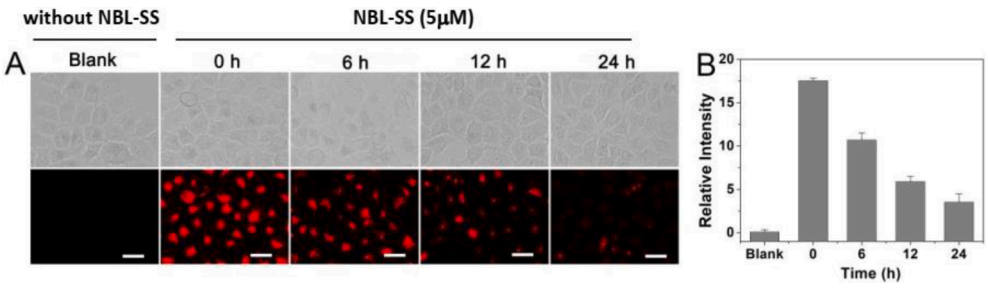

Fig. 4. Imaging Trx activity in HeLa cells. (A) Imaging the cellular Trx activity by NBL-SS (5 μM). HeLa cells were treated with **68** (10 μM) at different times, and the activity of Trx was stained by the probe NBL-SS for 5 min, the blank control was not stained by NBL-SS. The bright-field pictures (top panel) and the fluorescence pictures (bottom panel) were acquired by an inverted fluorescence microscope. Scale bars: 20 μm. The fluorescence intensity analysis of (A) by ImageJ was shown in (B).

activity has changed. Then we used the PAO-sepharose drop-down assay developed by our group to determine the redox status of Trx in HeLa cells were treated with **68** [44,45]. This assay has been further verified in previous studies by our group [46]. As shown in Fig. 5**A**, when the cells were treated with **68** (40 μM), the oxidized Trx increased significantly. Compared to the control group (non-**68** treated cells), Trx was mainly presented in the reduced form. Then the oxidized and reduced Trx was quantified by Image J, and the ratio of reduced Trx to oxidized Trx decreased significantly (Fig. 5**C**). As shown in Fig. 5**B**, the total expression of Trx decreased significantly, indicating that Trx was irreversibly inhibited by **68** [47]. These results showed that Trx was inhibited by compound **68** irreversibly.

2.7. Induction of ROS in cells

Trx system plays an important role in maintaining the intracellular redox homeostasis and resisting oxidative stress. Thus, Trx is inhibited by **68** might disturb the cellular redox balance and cause the accumulation of ROS in cells. The production of ROS in cells was detected by DCFH-DA. A weak fluorescence signal in the control group was detected indicating the presence of low-level ROS. After the HeLa cells were treated by the **68**, a bright green fluorescence became brighter as the concentration of **68** increased (Fig. 6**A**). Because of the limitation of DCFH-DA [48], we used another probe DHE to further detect ROS in cells. Unsurprisingly, **68**-treated cells promoted the fluorescence in a dose-dependent manner (Fig. 6**B**). In addition, we performed a quantitative analysis of fluorescence signal (Fig. 6**C and D**). Taken together, compound **68** promoted the production of ROS in HeLa cells.

2.8. Apoptosis induction by compound *68*

Once Trx was inhibited by small molecules, it would inevitably produce a large amount of ROS, induce oxidative stress, and eventually promote cancer cell death. Although the above studies showed that compound **68** could effectively inhibit Trx activity and elicit the accumulation of ROS in HeLa cells, we could not confirm that compound **68** induces oxidative stress-mediated apoptosis of HeLa cells. Therefore, the apoptosis was evaluated Annexin VFITC/PI double staining assay and caspase-3 activity test. Herein, we investigated the activity of caspase-3 after HeLa cells were incubated with **68** for 48 h. As shown in Fig. 7**C**, compound **68** activated caspase-3 in a concentration-dependent manner, indicating that compound **68** induced apoptosis in HeLa cells. Then, we applied the Annexin VFITC/PI double staining assay to quantify the apoptotic population by flow cytometer. The dot plots and the quantification results were shown in Fig. 7**A & B**. As the concentration of compound **68** enhanced, the number of apoptotic cells increased significantly. All these results indicated that **68** killed HeLa cells mainly by inducing apoptosis.

Trx plays an important role in many physiological and pathological processes including multiple stages of cancer. Compared to normal cell lines, tumor cell lines usually harbor elevated ROS as a result of their uncontrolled proliferation and high metabolic rate. To maintain the redox balance, cancer cells also upregulate the antioxidant system to eliminate ROS. Many studies have shown that many tumor cell lines with a high level of ROS and Trx [49]. Trx overexpressed in cancer cells is inhibited by inhibitors, and a large amount of ROS would futher accumulate in the cells, leading to the death of cancer cells [27,28,50]. Therefore, the development of anticancer drugs with Trx inhibition is a promising tumor treatment strategy.

Disulfide bond has good reactivity and biological activity and is an important functional group in various chemical and biological preparations. The exchange reaction between free thiol and disulfide bond plays a very important role in the redox cycle of the Trx system [29,30].

To develop an anticancer candidate with Trx inhibition, we synthesized a number of disulfides. Herein, we established a method for screening Trx inhibitors by using NBL-SS, a highly selective fluorescent probe for Trx developed by our group. This method reduced the workload of screening inhibitors greatly (Fig. 1). Combined with previous SAR studies [26,31], our studies showed that the symmetric disulfides can oxidize pure *E.coli* Trx, but they have low cytotoxicity. However, asymmetric disulfides not only oxidized Trx well but also had high cytotoxicity. We found that half of the molecule is an aromatic group with electron-withdrawing substituents showing better cytotoxicity. Therefore, compound **68** is an ideal molecule for further investigation. In addition, the results of the kinetic study further indicate that compound **68** has excellent interaction with *E. coli* Trx, we thus have further studied the intracellular behavior of compound **68**.

The effect of compound **68** on HeLa cells was demonstrated by the following evidence. First, we imaged the activity of Trx in HeLa cells by NBL-SS. The activity of Trx was inhibited by **68** in HeLa cells under our

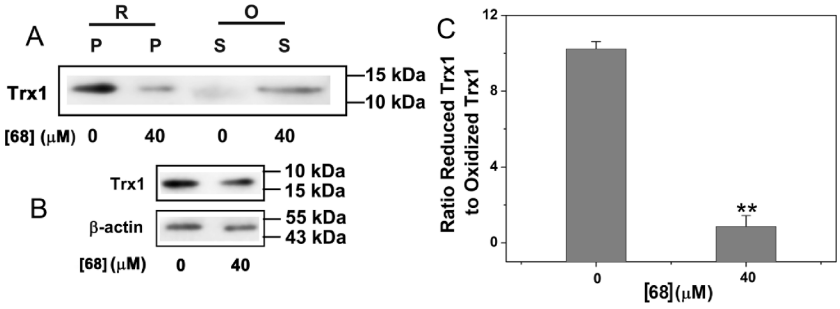

Fig. 5. Alteration of Trx redox status in HeLa cells. (A) Measurement of the oxidized Trx1 and reduced Trx1 by the PAO-sepharose assay. After treatment of HeLa cells with **68** (40 μM) for 48 h, the redox states of Trx1 were determined. S, samples in the supernatant; P, samples eluted from the PAO-sepharose beads; R, reduced form; O, oxidized form. (B) There was a significant change in Trx1 protein expression after being treated with **68**. After treatment of HeLa cells with **68** for 48 h, Western blot was performed to detect the expression of Trx1 protein. (C) The ratio of reduced/oxidized Trx1 was evaluated by ImageJ. ** $P < 0.01$ vs. the control groups in (C).

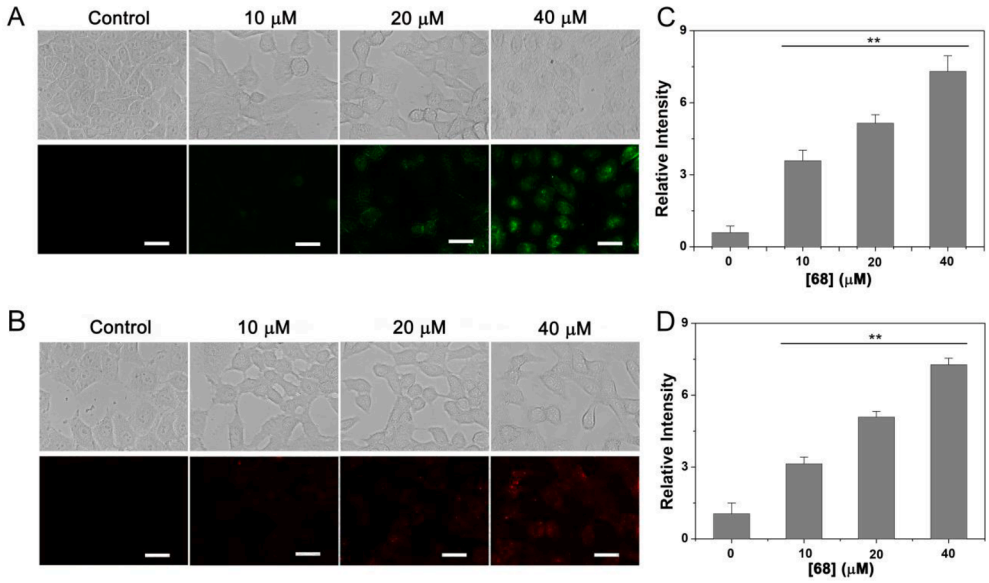

Fig. 6. Induction of oxidative stress by **68** in HeLa cells. HeLa cells were treated with varying concentrations of **68** for 12 h and were continued to incubate with (A) DCFH-DA (10 μM) or (B) DHE (10 μM) for 30 min. The pictures were acquired by an inverted fluorescence microscope. Scale bars: 20 μm. The fluorescence intensity analysis of (A) and (B) by ImageJ was shown in (C) and (D). Data are expressed as mean ± SE from triplicates. ** $P < 0.01$ vs. the control groups in (C) and (D).

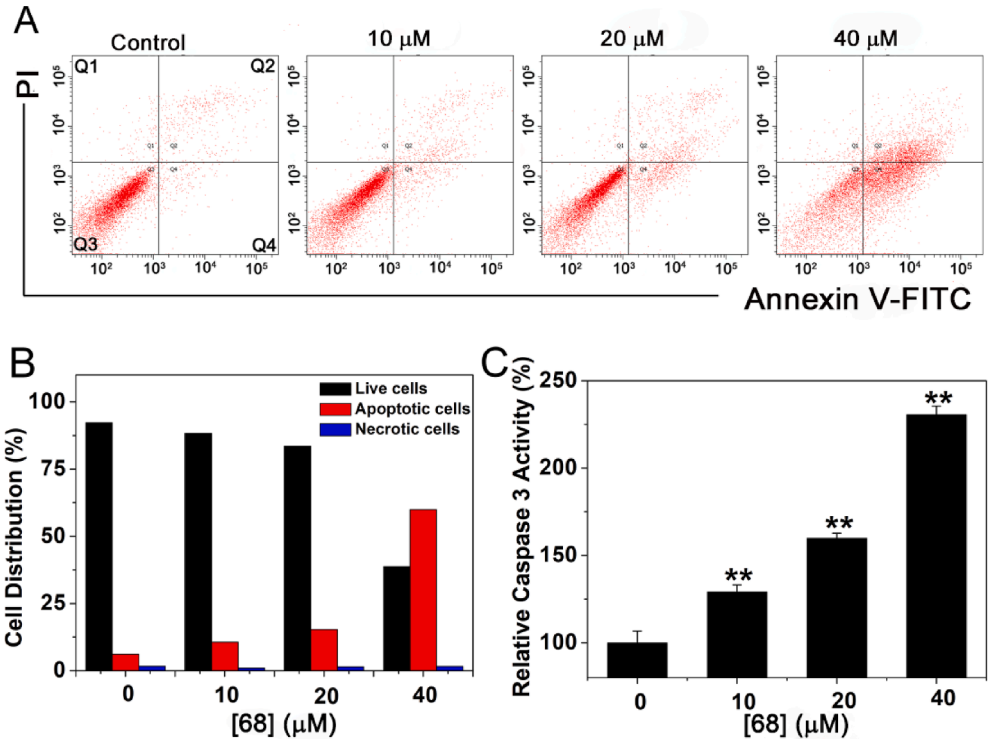

Fig. 7. Induction of apoptosis by **68** in HeLa cells. (A) Flow cytometric analysis of apoptosis by Annexin V/PI double staining assay in HeLa cells. HeLa cells were treated with different concentrations of **68** for 48 h and the population of live cells, apoptotic cells, and necrotic cells were analyzed by flow cytometry. The cells displayed four different groups marked as follows: PI-positively and FITC-negatively stained cells showing necrotic cells (upper left, Q1), double-negative (unstained) cells showing live cells (lower left, Q3), FITC-positively and PI-negatively stained cells showing early apoptosis (lower right, Q4) and FITC and PI double-stained cells showing late apoptosis (upper right, Q2). (B) Quantification of necrotic cells (Q1), apoptotic cells (Q2 and Q4), and live cells (Q3) were illustrated. (C) Activation of caspase-3 by **68** in HeLa cells. HeLa cells were treated with the indicated concentrations of **68** for 48 h and the activity of caspase-3 in the cell extracts was determined by a colorimetric assay. Data are expressed as mean ± SE from triplicates. ** $P < 0.01$ vs. the control groups in (C).

experimental conditions (Fig. 4). Since **68** could act as a Trx inhibitor by oxidizing Trx, the redox state of Trx in the HeLa cell is then tested (Fig. 5). These results showed that Trx was inhibited by compound **68**, and this may be similar to the established mechanism [31,35-37]. Trx inhibition by **68** disturbs the cellular redox balance, leading to the accumulation of ROS in cells (Fig. 6) and promoting cancer cell death eventually (Fig. 7).

3. Conclusion

In summary, 72 disulfides were synthesized and evaluated for antitumor activity in HeLa cells. We established an efficient and fast method to screen Trx inhibitors by using the probe NBL-SS and found compound **68** had the greatest potential as a candidate for Trx inhibitors. In addition, studies demonstrated that **68** impinged on the Trx system *via* inhibition of Trx, which induced oxidative stress and eventually led to apoptosis of HeLa cells. The SAR analysis would facilitate our further optimization disulfides to develop anticancer candidates with Trx inhibition.

4. Experimental section

4.1. Materials and instruments

The recombinant *E. coli* Trx was prepared according to our established protocol, and the purity of the protein was > 95% judged by Coomassie-stained SDS-polyacrylamide gel electrophoresis (PAGE) [39]. HepG2, HeLa, HEK 293T, and BEAS-2B cells were obtained from the Shanghai Institute of Biochemistry and Cell Biology, Chinese Academy of Sciences. RPMI 1640 medium, Dulbecco's modified Eagle medium (DMEM), DL-dithiothreitol (DTT), dimethyl sulfoxide (DMSO), were obtained from Roche (Mannheim, Germany). 3-(4, 5-Dimethylthiazol-2-yl)-2,5-diphenyltetrazolium bromide (MTT; Amresco, Solon, USA). The primary antibodies against Trx1 and β-actin were from Sangon Biotech (Shanghai, China). ^{1}H NMR and ^{13}C NMR spectra were recorded on a Bruker AMX spectrometer at 400 and 100 MHz in deuterated solvents, respectively, and tetramethylsilane (TMS) was used as a reference (chemical shifts are given in δ values, J is given in Hz). Mass spectra were obtained using a Hewlett-Packard 5988A spectrometer or a Shimadzu LC-MS-2020 system. The purity of all final compounds was assessed by HPLC. All other reagents were purchased from commercial supplies. All reactions were monitored using thin-layer chromatography (TLC) on commercial silica-gel plates (GF254). Visualization of the developed plates was performed under UV light (254 nm). Flash column chromatography was performed on silica gel (200–300 mesh). Fluorescence studies were carried out using a Cary Eclipse Fluorescence spectrophotometer (Agilent Technologies). The fluorescence images of the cells were acquired on a Floid cell imaging station (life technology) or an inverted fluorescent microscope (Leica DMI4000). The absorbance was measured on Multiskan GO (Thermo Scientific) or Microplate Reader (FlexStation 3, USA). The gel images were acquired with a Gel imager (G: BOX Chemi XX9, Syngene, UK). The data of Annexin V/PI staining were determined by a FACSCanto™ flow cytometer (BD Biosciences, USA).

4.2. Compounds purity analysis

The purity of all compounds was determined by HPLC. The analyses were performed on the Shimadzu LC-MS-2020 system with a Wondasil C18 Superb reversed-phase column (5 mm, 4.6 mm × 150 mm). The mobile phase was methanol and water, and the flow rate was 0.6 mL/min. All tested compounds were dissolved in methanol, and the injection volume was 5 μL. The maximum absorbance range of the detection wavelength was 210–400 nm. The purity of target compounds was higher than 95%, except compounds **9, 64, 72**, whose purity is 94.0%, 94.2% and 94.1%, respectively.

4.3. Target compounds synthesis and characterization

Compounds **1**–**14** were synthesized following the method described by Sun, L. *et al.* [40].

Synthesis of compound **1.** Thiophenol (440 mg, 4 mmol) was added to a flask and dissolved in anhydrous dichloromethane (DCM, 50 mL), sodium bicarbonate (420 mg, 5 mmol) was added to the flask with vigorous stirring at room temperature. After stirring for 15 min, iodine (1.5 g, 6 mmol) was added to the reaction mixture slowly and stirred for an additional 30 min vigorously. Then, add saturated aqueous $Na_2S_2O_3$ to the reaction mixture to remove excess iodine, until the solution turns colorless. The resulting mixture was extracted with DCM. The organic phase was dried over anhydrous $MgSO_4$, filtered, evaporated under reduced pressure and purified with column chromatography by using petroleum ether/ethyl acetate as eluent to give the desired product. Compounds **2**–**14** were prepared by the method used for compound **1.**

Compounds **15**–**53** were synthesized following the method by Stellenboom, N. *et al.* [41].

Synthesis of compound **15.** 1-Chlorobenzotriazole (610 mg, 4 mmol) and 1H-Benzotriazole (320 mg, 2.7 mmol) was added to a flask and dissolved in anhydrous dichloromethane (DCM, 30 mL), then 4-Fluorothiophenol as R^1SH (346 mg, 2.7 mmol) was dissolved in DCM (2 mL) and was added dropwise under Ar atmosphere at −78 °C. After stirring for 2 h with slow warming to −20 °C, 1-Propanethiol (304 mg, 4 mmol) as R^2SH in DCM (2 mL) was added to the reaction mixture slowly at −20 °C and was continuously stirred for 30 min at 0 °C. The reaction was then quenched with a solution of $Na_2S_2O_3$ (0.50 g in 10 mL water) together with saturated aqueous $NaHCO_3$ (20 mL). The resulting mixture was extracted with DCM. The organic phase was dried over anhydrous $MgSO_4$, filtered, evaporated under reduced pressure and purified with column chromatography by using petroleum ether/ethyl acetate as eluent to give the desired product. Compounds **16**–**53** were prepared by the method used for **15.**

Compounds **54**–**72** were synthesized following the method by Khosla, C. *et al.* [31].

Intermediate **s54** was obtained from commercially available sources. Cyclohexyl mercaptan (754 mg, 6.5 mmol) and thiourea (380 mg, 5 mmol) were dissolved in H_2O-ethanol (40 mL, 1:3 mixture). Then concentrated hydrochloric acid (2 mL) was added to the reaction mixture carefully under an ice-water bath·H_2O_2 (30%, 0.9 mL) was added dropwise with vigorous stirring and was continually stirred at 0 °C for 3 h. The solvent was evaporated under reduced pressure and collected the crude intermediates. All intermediates were prepared by the method used for **s54.**

Synthesis of compound **54**. 2-Mercaptobenzoxazole (332 mg, 2.2 mmol) and **s54** (565 mg, 2.5 mmol) were dissolved in methanol (6 mL). $NaHCO_3$ (286 mg, 3.4 mmol) in water (10 mL) was added dropwise with vigorous stirring at room temperature for 1 h. The resulting mixture was diluted with water, and was extracted with DCM. The organic phase was dried over anhydrous $MgSO_4$, filtered, evaporated under reduced pressure and purified with column chromatography by using petroleum ether/ethyl acetate as eluent to give the desired product. Compounds **55**–**72** were prepared by the method used for **54.**

Diphenyl disulfide (1). Yield: 85.7%; ^{1}H NMR (400 MHz, $CDCl_3$) δ 7.508–7.490 (m, 4H), 7.325–7.285 (m, 4H), 7.245–7.208 (m, 2H). ^{13}C NMR (100 MHz, $CDCl_3$) δ 137.16, 129.21, 127.63, 127.30. MS-APCI *m/z*: 242.0 $[M + Na]^+$. HPLC analysis: Rt = 8.11 min, purity 97.87%, 90:10 CH_3OH/H_2O.

Bis(4-methoxyphenyl) disulfide (2). Yield: 82.3%; ^{1}H NMR (400 MHz, $CDCl_3$) δ 7.413 (d, J = 6.4 Hz, 4H), 6.852 (d, J = 8.8 Hz, 4H), 3.814 (s, 6H). ^{13}C NMR (100 MHz, $CDCl_3$) δ 160.04, 132.80, 128.55, 114.74. MS-APCI *m/z*: 278.0 $[M + H]^+$. HPLC analysis: Rt = 4.09 min, purity 99.49%, 90:10 CH_3OH/H_2O.

Bis(2-methoxyphenyl) disulfide (3). Yield: 90.9%; ^{1}H NMR (400 MHz, $CDCl_3$) δ 7.531 (d, J = 6.4 Hz, 2H), 7.187 (t, J = 1.6 Hz, 2H), 6.913 (t, J = 3.8 Hz, 2H), 6.855(d, J = 7.2 Hz, 2H). ^{13}C NMR (100 MHz, $CDCl_3$) δ 156.67, 127.85, 127.64, 124.64, 121.44, 110.59, 55.98. MS-APCI *m/z*: 279.0 $[M + H]^+$. HPLC analysis: Rt = 6.548 min, purity 97.61%, 90:10 CH_3OH/H_2O.

Bis(2-aminophenyl) disulfide (4). Yield: 88.3%; ^{1}H NMR (400 MHz, $CDCl_3$) δ 7.179–7.137 (m, 4H), 6.726–6.706 (m, 2H), 6.605–6.567 (m, 2H). ^{13}C NMR (100 MHz, $CDCl_3$) δ 148.72, 136.91, 131.70, 118.80, 118.31, 115.33. MS-ESI *m/z*: 248.9 $[M + H]^+$. HPLC analysis: Rt = 10.41 min, purity 95.68%, 80:20 CH_3OH/H_2O.

Bis(4-aminophenyl) disulfide (5). Yield: 83.9%; ^{1}H NMR (400 MHz, $CDCl_3$) δ 7.276 (d, J = 6.8 Hz, 4H), 6.618 (d, J = 7.2 Hz, 4H). ^{13}C NMR (100 MHz, $CDCl_3$) δ 178.07, 161.23, 132.12, 130.78, 116.23, 33.66, 32.76. MS-ESI *m/z*: 248.9 $[M + H]^+$. HPLC analysis: Rt = 7.89 min, purity 99.18%, 90:10 CH_3OH/H_2O.

4,4′-Dithiobisbenzoic acid (6). Yield: 91.1%; ^{1}H NMR (400 MHz, DMSO-d_6) δ 7.932 (d, J = 8.8 Hz, 4H), 7.638 (d, J = 8.4 Hz, 4H). ^{13}C NMR (100 MHz, DMSO-d_6) δ 166.732, 140.778, 130.386, 129.823, 126.114. MS-ESI *m/z*: 611.3 $[2M-H]^-$. HPLC analysis: Rt = 10.18 min, purity 95.13%, 80:20 CH_3OH/H_2O.

Bis(4-methylphenyl) disulfide (7). Yield: 84.6%; ^{1}H NMR (400

MHz, $CDCl_3$) δ 7.187 (d, J = 8.4 Hz, 4H), 7.052 (d, J = 8.0 Hz, 4H). ^{13}C NMR (100 MHz, $CDCl_3$) δ 135,729, 129.935, 128.580, 126.676. MS-APCI m/z: 246.0 $[M]^+$. HPLC analysis: Rt = 6.575 min, purity 99.56%, 90:10 CH_3OH/H_2O.

Bis(4-hydroxyphenyl) disulfide (8). Yield: 88.1%; ^1H NMR (400 MHz, DMSO-d_6) δ 9.842 (s, 2H), 7.268 (d, J = 8.8 Hz, 4H), 6.754 (d, J = 8.8 Hz). ^{13}C NMR (100 MHz, DMSO-d_6) δ 158.32, 133.10, 125.14, 116.36. MS-ESI m/z: 499.5 $[2M-H]^-$. HPLC analysis: Rt = 10.54 min, purity 98.89%, 75:25 CH_3OH/H_2O.

Bis(3-chlorophenyl) disulfide (9). Yield: 88.9%; ^1H NMR (400 MHz, $CDCl_3$) δ 7.474–7.134 (m, 8H). ^{13}C NMR (100 MHz, DMSO-d_6) δ 138.14, 134.44, 131.56, 128.10, 126.77, 126.09. MS-APCI m/z: 285.0 $[M-2H]^-$. HPLC analysis: Rt = 9.60 min, purity 94.00%, 75:25 CH_3OH/H_2O.

Bis(2-chlorophenyl) disulfide (10). Yield: 82.9%; ^1H NMR (400 MHz, $CDCl_3$) δ 7.546 (d, J = 6.4 Hz, 2H), 7.366 (d, J = 6.8 Hz, 2H), 7.226 (t, J = 7.0 Hz, 2H), 7.163 (t, J = 7.0 Hz, 2H). ^{13}C NMR (100 MHz, DMSO-d_6) δ 133.46, 131.69, 130.55, 129.61, 128.95, 128.15. MS-APCI m/z: 285.0 $[M-2H]^-$. HPLC analysis: Rt = 3.05 min, purity 95.58%, 90:10 CH_3OH/H_2O.

Bis(4-fluorodiphenyl) disulfide (11). Yield: 79.8%; ^1H NMR (400 MHz, $CDCl_3$) δ 7.400 (d, J = 8.4 Hz, 4H), 7.277 (d, J = 8.8 Hz, 4H). ^{13}C NMR (100 MHz, $CDCl_3$) δ 161.48, 132.27, 131.33, 116.54. MS-APCI m/z: 253.0 $[M-H]^-$. HPLC analysis: Rt = 13.24 min, purity 98.64%, 90:10 CH_3OH/H_2O.

Bis(1H-benzimidazol) disulfide (12). Yield: 78.9%; ^1H NMR (400 MHz, DMSO-d_6) δ 7.518 (q, J = 8.8, 4H), δ 7.203 (d, J = 2.8 Hz, 4H). ^{13}C NMR (100 MHz, DMSO-d_6) δ 147.78, 140.16, 132.68, 123.07, 122.79, 155.59, 109.94. MS-ESI m/z: 298.8 $[M + H]^+$. HPLC analysis: Rt = 13.74 min, purity 98.90%, 80:20 CH_3OH/H_2O.

Dibenzoxazolyl disulfide (13). Yield: 80.4%; ^1H NMR (400 MHz, DMSO-d_6) δ 7.544 (s, 2H), 7.238 (m, 2H), 2.975 (m, 1H), 1.762 (m, 1H), 1.567 (m, 1H) 1.326 (d, J = 6.8 Hz, 3H) 0.968 (t, J = 7.6 Hz, 3H). ^{13}C NMR (100 MHz, DMSO-d_6) δ 180.58, 148.58, 131.63, 125.57, 124.20, 110.91, 110.41. MS-APCI m/z: 301.0 $[M + H]^+$. HPLC analysis: Rt = 3.82 min, purity 99.11%, 90:10 CH_3OH/H_2O.

Bis(5-methoxy-1H-benzimidazol) disulfide (14). Yield: 78.4%; ^1H NMR (400 MHz, $CDCl_3$) δ 7.595 (d, J = 8.8 Hz, 2H), 7.127 (d, J = 1.2 Hz, 2H), 6.984 (d, J = 8.8 Hz, 2H), 3.884 (s, 6H). ^{13}C NMR (100 MHz, $CDCl_3$) δ 156.72, 140.51, 138.93, 132.71, 116.18, 112.78, 96.99, 55.97. MS-ESI m/z: 239.8 $[M + H]^+$. HPLC analysis: Rt = 6.52 min, purity 97.49%, 85:15 CH_3OH/H_2O.

4-Fluorophenyl propyl disulfide (15). Yield: 79.1%; ^1H NMR (400 MHz, $CDCl_3$) δ 7.526–7.491 (m, 2H), 7.044–7.000 (m, 2H), 2.726 (t, J = 7.2 Hz, 2H), 1.756–1.646 (m, 2H), 0.963 (t, J = 7.2 Hz, 3H). ^{13}C NMR (100 MHz, $CDCl_3$) δ 161.040, 133.063, 130.345, 116.068, 41.041, 22.251, 13.201. MS-APCI m/z: 201.0 $[M-H]^-$. HPLC analysis: Rt = 14.75 min, purity 95.08%, 80:20 CH_3OH/H_2O.

4-Fluorophenyl 2-allyl disulfide (16). Yield: 90.2%; ^1H NMR (400 MHz, $CDCl_3$) δ 7.523–7.488 (m, 2H), 7.023 (t, J = 8.8 Hz, 2H), 5.852–5.748 (m, 1H), 5,180–5.129 (m, 2H), 3.358 (d, J = 7.2 Hz, 2H). ^{13}C NMR (100 MHz, $CDCl_3$) δ 161.163, 132.657, 131.009, 119.277, 116.084, 41.895. MS-APCI m/z: 201.0 $[M + H]^+$. HPLC analysis: Rt = 12.10 min, purity 95.87%, 80:20 CH_3OH/H_2O.

4-Fluorophenyl *tert*-butyl disulfide (17). Yield: 75.2%; ^1H NMR (400 MHz, $CDCl_3$) δ 7.540–7.505 (m, 2H), 6.993 (t, J = 8.8 Hz, 2H), 1.291 (s, 9H). ^{13}C NMR (100 MHz, $CDCl_3$) δ 163.12, 134.17, 129.36, 116.07, 49.43, 29.96. MS-APCI m/z: 217.0 $[M + H]^+$. HPLC analysis: Rt = 11.86 min, purity 95.05%, 80:20 CH_3OH/H_2O.

4-Fluorophenyl 2-pyridyl disulfide (18). Yield: 77.3%; ^1H NMR (400 MHz, $CDCl_3$) δ 8.489 (d, J = 4.8 Hz, 1H), 7.653–7.636 (m, 2H), 7.535–7.500 (m, 1H), 7.459–7.424 (m, 1H), 7.127–7.116 (m, 1H), 7.025–6.987 (m, 2H). ^{13}C NMR (100 MHz, $CDCl_3$) δ 163.81, 159.47, 149.84, 137.54, 131.36, 130.41, 121.24, 119.87, 116.53. MS-APCI m/z: 238.0 $[M + H]^+$. HPLC analysis: Rt = 13.85 min, purity 99.08%, 80:20 CH_3OH/H_2O.

4-Fluorophenyl 4-methylphenyl disulfide (19). Yield: 75.5%; ^1H NMR (400 MHz, $CDCl_3$) δ 7.473–7.438 (m, 1H), 7.394–7.361 (m, 2H), 7.129–7.109 (m, 2H), 7.094–6.972 (m, 1H), 2.326 (d, J = 4.0 Hz, 3H). ^{13}C NMR (100 MHz, $CDCl_3$) δ 161.26, 137.94, 133.51, 130.83, 130.01, 128.98, 128.58, 116.15, 21.21. MS-APCI m/z: 249.0 $[M-H]^-$. HPLC analysis: Rt = 8.44 min, purity 97.35%, 85:15 CH_3OH/H_2O.

4-Fluorophenyl cyclopentyl disulfide (20). Yield: 84.7%; ^1H NMR (400 MHz, $CDCl_3$) δ 7.531–7.496 (m, 2H), 7.014 (t, J = 8.8 Hz, 2H), 3.343–3.294 (m, 1H), 1.980–1.915 (m, 3H), 1.746–1.669 (m, 5H). ^{13}C NMR (100 MHz, $CDCl_3$) δ 160.87, 133.34, 133.31, 129.94, 116.20, 50.40, 32.82, 24.80. MS-APCI m/z: 229.0 $[M + H]^+$. HPLC analysis: Rt = 6.73 min, purity 95.58%, 85:15 CH_3OH/H_2O.

2-[2-(4-Fluorophenyldisulfanyl)] benzoic acid (21). Yield: 85.4%; ^1H NMR (400 MHz, $CDCl_3$) δ 8.158 (d, J = 6.4 Hz, 1H), 8.078 (d, J = 7.6 Hz, 1H), 7.576 (t, J = 7.0 Hz, 1H), 7.478–7.443 (m, 2H), 7.320 (d, J = 0.8 Hz, 1H), 6.992 (t, J = 8.8 Hz, 2H). ^{13}C NMR (100 MHz, DMSO-d_6) δ 167.75, 139.59, 133.39, 131.69, 131.11, 129.94, 127.66, 126.12, 124.97, 116.72. MS-ESI m/z: 279 $[M-H]^-$. HPLC analysis: Rt = 7.57 min, purity 98.63%, 85:25 CH_3OH/H_2O.

4-Fluorophenyl isopropyl disulfide (22). Yield: 83.1%; ^1H NMR (400 MHz, $CDCl_3$) δ 7.527–7.492 (m, 2H), 7.008 (t, J = 8.8 Hz, 2H), 3.104–3.003 (m, 1H), 1.292 (d, J = 6.8 Hz, 6H). ^{13}C NMR (100 MHz, $CDCl_3$) δ 160.80, 133.52, 129.86, 115.95, 41.65, 22.46. MS-APCI m/z: 203.0 $[M + H]^+$. HPLC analysis: Rt = 12.40 min, purity 96.41%, 80:20 CH_3OH/H_2O.

2-[2-(4-Fluorophenyldisulfanyl)] methyl acetate (23). Yield: 69.6%; ^1H NMR (400 MHz, $CDCl_3$) δ 7.556–7.521 (m, 2H), 7.063–7.020 (m, 2H), 3.608 (s, 3H), 3.494 (s, 2H). ^{13}C NMR (100 MHz, $CDCl_3$) δ 169.40, 163.90, 131.94, 131.85, 116.18, 52.54, 40.57. MS-APCI m/z: 233.0 $[M + H]^+$. HPLC analysis: Rt = 7.61 min, purity 96.09%, 85:15 CH_3OH/H_2O.

3-[2-(4-Methylphenyldisulfanyl)] propionic acid (24). Yield: 70.2%; ^1H NMR (400 MHz, $CDCl_3$) δ 7.478 (d, J = 8.8 Hz, 1H), 7.396 (d, J = 8.8 Hz, 1H), 6.873–6.822 (m, 2H), 3.086 (s, 3H), 2.725–2.649 (m, 2H), 1.738–1.674 (m, 2H), 1.013–0.940 (m, 3H). ^{13}C NMR (100 MHz, $CDCl_3$) δ 159.51, 131.68, 128.56, 114.67, 55.47, 40.83, 22.15, 13.23. MS-APCI m/z: 214.0 $[M + H]^+$. HPLC analysis: Rt = 5.66 min, purity 98.01%, 90:10 CH_3OH/H_2O.

4-Methylphenyl 2-pyridyl disulfide (25). Yield: 84.9%; ^1H NMR (400 MHz, $CDCl_3$) δ 7.477 (d, J = 8.8 Hz, 2H), 6.849 (d, J = 8.8 Hz, 2H), 3.801 (s, 3H), 2.858–2.774 (m, 1H), 1.760–1.654 (m, 1H), 1.561–1.453 (m, 1H), 1.274 (d, J = 6.8 Hz, 3H), 0.917 (t, J = 7.2 Hz, 3H). ^{13}C NMR (100 MHz, $CDCl_3$) δ 159.27, 131.10, 129.25, 114.59, 55.46, 48.28, 28.79, 19.97, 11.52. MS-APCI m/z: 228.0 $[M + H]^+$. HPLC analysis: Rt = 9.47 min, purity 97.04%, 85:15 CH_3OH/H_2O.

4-Methylphenyl propyl disulfide (26). Yield: 87.7%; ^1H NMR (400 MHz, $CDCl_3$) δ 7.488 (d, J = 8.8 Hz, 2H), 6.837 (d, J = 8.8 Hz, 2H), 3.794 (s, 3H), 1.290 (s, 9H). ^{13}C NMR (100 MHz, $CDCl_3$) δ 158.92, 130.28, 129.73, 114.45, 55.37, 48.99, 29.95. MS-APCI m/z: 229.0 $[M + H]^+$. HPLC analysis: Rt = 3.01 min, purity 97.73%, 90:10 CH_3OH/H_2O.

4-Methylphenyl isopropyl disulfide (27). Yield: 86.5%; ^1H NMR (400 MHz, $CDCl_3$) δ 7.681–7.658 (m, 1H), 7.230 (d, J = 0.8 Hz, 1H), 7.030 (t, J = 7.4 Hz, 1H), 6.863 (d, J = 8.0 Hz, 1H), 3.891 (s, 3H), 3.678 (s, 3H), δ 2.956 (t, J = 7.2 Hz, 2H), 2.761 (t, J = 7.2 Hz, 2H). ^{13}C NMR (100 MHz, $CDCl_3$) δ 172.26, 156.81, 128.29, 128.23, 124.68, 121.28, 110.76, 55.89, 51.91, 33.65, 32.82. MS-APCI m/z: 259.0 $[M + H]^+$. HPLC analysis: Rt = 14.59 min, purity 97.94%, 80:20 CH_3OH/H_2O.

4-Methylphenyl 1-methylpropyl disulfide (28). Yield: 80.3%; ^1H NMR (400 MHz, $CDCl_3$) δ 7.649 (d, J = 8.0 Hz, 1H), 7.256 (d, J = 8.0 Hz, 1H), 6.978 (t, J = 7.6 Hz, 1H), 6.879 (d, J = 8.0 Hz, 1H), 3.895 (s, 3H), 3.634 (s, 3H), 3.542 (s, 2H). ^{13}C NMR (100 MHz, $CDCl_3$) δ 170.04, 156.69, 129.35, 128.77, 127.23, 123.42, 121.77, 111.78, 56.41, 52.70, 40.50. MS-APCI m/z: 245.0 $[M + H]^+$. HPLC analysis: Rt = 6.56 min, purity 95.94%, 85:15 CH_3OH/H_2O.

4-Methylphenyl 2-allyl disulfide (29). Yield: 83.8%; ^1H NMR (400 MHz, $CDCl_3$) δ 8.454 (d, J = 4.0 Hz, 1H), 7.675–7.652 (m, 1H),

7.599–7.595 (m, 1H), 7.538–7.515 (m, 1H), 7.239–7.214 (m, 1H) , 7.200–2.196 (m, 1H), 7.095–7.062 (m, 1H), 6.918–6.883 (m, 1H), 3.902 (s, 3H). ^{13}C NMR (100 MHz, $CDCl_3$) δ 158.95, 156.58, 149.66, 137.52, 128.38, 127.81, 124.51, 121.41, 120.81, 119.70, 110.51, 55.96. MS-APCI *m/z*: 250.0 $[M + H]^+$. HPLC analysis: Rt = 6.06 min, purity 97.52%, 85:15 CH_3OH/H_2O.

4-Methylphenyl cyclopentyl disulfide (30). Yield: 74.1%; ^{1}H NMR (400 MHz, $CDCl_3$) δ 7.715 (d, J = 6.0 Hz, 1H), 7.189 (t, J = 7.6 Hz, 1H), 6.988 (t, J = 7.6 Hz, 1H), 6.845 (d, J = 8.4 Hz, 1H), 3.898 (s, 3H), 3.108–3.007 (m, 1H), 1.313 (d, J = 2.8 Hz, 6H). ^{13}C NMR (100 MHz, $CDCl_3$) δ 156.35, 127.43, 126.06, 121.20, 110.60, 55.94, 41.28, 22.53. MS-APCI *m/z*: 215.0 $[M + H]^+$. HPLC analysis: Rt = 7.85 min, purity 98.62%, 85:15 CH_3OH/H_2O.

4-Methylphenyl *tert*-butyl disulfide (31). Yield: 85.2%; ^{1}H NMR (400 MHz, $CDCl_3$) δ 7.670 (d, J = 6.0 Hz, 1H), 7.239 (t, J = 1.6 Hz, 1H), 6.998 (t, J = 3.6 Hz, 1H), 6.878 (d, J = 0.8 Hz, 1H), 3.892 (s, 3H), 2.952 (t, J = 7.0 Hz, 2H), 2.823 (t, J = 7.0 Hz, 2H). ^{13}C NMR (100 MHz, $CDCl_3$) δ 178.50, 156.92, 128.57, 128.43, 124.50, 121.32, 110.82, 55.89, 33.71, 32.34. MS-ESI *m/z*: 287.3[2 M−H]$^-$. HPLC analysis: Rt = 8.31 min, purity 96.64%, 85:15 CH_3OH/H_2O.

4-Methylphenyl cyclohexyl disulfide (32). Yield: 74.2%; ^{1}H NMR (400 MHz, $CDCl_3$) δ 7.432 (d, J = 8.8 Hz, 2H), 6.781 (d, J = 8.4 Hz, 2H), 2.859–2.775 (m, 1H), 1.738–1.651 (m, 1H), 1.546–1.475 (m, 1H), 1.276 (d, J = 6.8 Hz, 3H), 0.919 (t, J = 7.2 Hz, 3H). ^{13}C NMR (100 MHz, $CDCl_3$) δ 155.13, 131.26, 129.40, 116.09, 48.30, 28.73, 19.90, 11.42. MS-APCI *m/z*: 213.0 [M−H]$^-$. HPLC analysis: Rt = 6.93 min, purity 98.15%, 85:15 CH_3OH/H_2O.

3-[2-(4-Methylphenyldisulfanyl)] methyl propionate (33). Yield: 78.7%; ^{1}H NMR (400 MHz, $CDCl_3$) δ 7.433 (d, J = 8.8 Hz, 2H), 6.783 (d, J = 8.8 Hz, 2H), 3.080–3.013 (m, 1H), 1.291 (d, J = 6.8 Hz, 6H). ^{13}C NMR (100 MHz, DMSO-d_6) δ 157.62, 131.80, 125.73, 116.21, 40.70, 22.14. MS-ESI *m/z*: 199.3 [M−H]$^-$. HPLC analysis: Rt = 11.24 min, purity 90.08%, 80:10 CH_3OH/H_2O.

2-[2-(4-Methylphenyldisulfanyl)] methyl acetate (34). Yield: 85.1%; ^{1}H NMR (400 MHz, $CDCl_3$) δ 7.425 (d, J = 8.0 Hz, 2H), 7.141 (d, J = 8.0 Hz, 2H), 2.941 (t, J = 6.6 Hz, 2H), 2.796 (t, J = 7.0 Hz, 2H), 2.338 (s, 3H). ^{13}C NMR (100 MHz, $CDCl_3$) δ 137.65, 133.33, 130.02, 128.84, 33.69, 32.63, 21.20. MS-ESI *m/z*: 454.5 [2 M−H]$^-$. HPLC analysis: Rt = 6.14 min, purity 97.81%, 85:15 CH_3OH/H_2O.

4-Methoxyphenyl propyl disulfide (35). Yield: 72.2%; ^{1}H NMR (400 MHz, $CDCl_3$) δ 8.460 (s, 2H), 7.675 (d, J = 8.0 Hz, 1H), 7.634–7.591 (m, 1H), 7.420 (d, J = 8.0 Hz, 2H), 7.110 (d, J = 7.6 Hz, 2H), 7.076 (d, J = 4.8 Hz, 1H), 2.312 (s, 3H). ^{13}C NMR (100 MHz, $CDCl_3$) δ 159.97, 149.57, 137.65, 137.30, 132.68, 129.97, 128.07, 120.85, 119.58, 21.11. MS-APCI *m/z*: 234.0 $[M + H]^+$. HPLC analysis: Rt = 3.46 min, purity 95.05%, 90:10 CH_3OH/H_2O.

4-Methoxyphenyl 1-methylpropyl disulfide (36). Yield: 81.6%; ^{1}H NMR (400 MHz, $CDCl_3$) δ 7.429 (d, J = 8.0 Hz, 2H), 7.130 (d, J = 8.0 Hz, 2H), 2.706 (t, J = 7.2 Hz, 2H), 2.335 (s, 3H), 1.743–1.652 (m, 2H), 0.964 (t, J = 7.2 Hz, 3H). ^{13}C NMR (100 MHz, $CDCl_3$) δ 137.01, 134.28, 129.82, 128.33, 40.91, 22.24, 21.15, 13.23. MS-APCI *m/z*: 196.0 [M−H]$^-$. HPLC analysis: Rt = 3.54 min, purity 95.33%, 90:10 CH_3OH/H_2O.

4-Methoxyphenyl *tert*-butyl disulfide (37). Yield: 83.3%; ^{1}H NMR (400 MHz, $CDCl_3$) δ 7.430 (d, J = 8.4 Hz, 2H), 7.115 (d, J = 8.0 Hz, 2H), 3.084–3.015 (m, 1H), 2.323 (s, 3H), 1.293 (d, J = 6.4 Hz, 6H). ^{13}C NMR (100 MHz, $CDCl_3$) δ 136.73, 134.87, 129.74, 127.91, 41.51, 22.50, 21.14. MS-APCI *m/z*: 221.0 $[M + Na]^+$. HPLC analysis: Rt = 13.28 min, purity 99.10%, 80:20 CH_3OH/H_2O.

3-[2-(2-Methoxyphenyldisulfanyl)] methyl propionate (38). Yield: 83.7%; ^{1}H NMR (400 MHz, $CDCl_3$) δ 7.430 (d, J = 8.4 Hz, 2H), 7.114 (d, J = 8.0 Hz, 2H), 2.863–2.779 (m, 1H), 2.326 (s, 3H), 1.747–1.678 (m, 1H), 1.548–1.480 (m, 1H), 1.284 (t, J = 6.4 Hz, 3H), 0.962 (t, J = 6.8 Hz, 3H). ^{13}C NMR (100 MHz, $CDCl_3$) δ 136.70, 134.92, 129.72, 127.93, 48.35, 28.84, 21.14, 19.97, 11.57. MS-APCI *m/z*: 213.0 $[M + H]^+$. HPLC analysis: Rt = 3.74 min, purity 95.0%, 90:10 CH_3OH/H_2O.

2-[2-(2-Methoxyphenyldisulfanyl)] methyl acetate (39). Yield: 80.6%; ^{1}H NMR (400 MHz, $CDCl_3$) δ 7.427 (d, J = 8.0 Hz, 2H), 7.133 (d, J = 8.0 Hz, 2H), 5.873–5.770 (m, 1H), 5.174–5.127 (m, 2H), 3.356 (d, J = 7.2 Hz, 2H), 2.339 (s, 3H). ^{13}C NMR (100 MHz, $CDCl_3$) δ 137.30, 133.81, 132.74, 129.83, 128.89, 119.08, 41.71, 21.18. MS-APCI *m/z*: 197.0 $[M + H]^+$. HPLC analysis: Rt = 8.11 min, purity 95.85%, 85:15 CH_3OH/H_2O.

2-Methoxyphenyl 2-pyridyl disulfide (40). Yield: 81.7%; ^{1}H NMR (400 MHz, $CDCl_3$) δ 7.435 (d, J = 8.4 Hz, 2H), 7.123 (d, J = 8.0 Hz, 2H), 3.358–3.278 (m, 1H), 2.330(s, 3H), 1.940–1.644 (m, 8H). ^{13}C NMR (100 MHz, $CDCl_3$) δ 136.70, 134.60, 129.71, 127.95, 50.25, 32.79, 24.79, 21.11. MS-APCI *m/z*: 225.0 $[M + H]^+$. HPLC analysis: Rt = 4.92 min, purity 96.93%, 90:10 CH_3OH/H_2O.

2-Methoxyphenyl isopropyl disulfide (41). Yield: 59.6%; ^{1}H NMR (400 MHz, $CDCl_3$) δ 7.444 (d, J = 8.4 Hz, 2H), 7.097 (d, J = 8.0 Hz, 2H), 2.316 (s, 3H), 1.297 (s, 9H). ^{13}C NMR (100 MHz, $CDCl_3$) δ 136.38, 135.42, 129.62, 127.44, 49.18, 29.97, 21.12. MS-APCI *m/z*: 213.0 $[M + H]^+$. HPLC analysis: Rt = 8.65 min, purity 95.15%, 85:15 CH_3OH/H_2O.

3-[2-(2-Methoxyphenyldisulfanyl)] propionic acid (42). Yield: 66.7%; ^{1}H NMR (400 MHz, $CDCl_3$) δ 7.425 (d, J = 8.4 Hz, 2H), 7.118 (d, J = 8.4 Hz, 2H), 2.828–2.756 (m, 1H), 2.328 (s, 3H), 2.030–1.993 (m, 2H), 1.778–1.740 (m, 2H), 1.370–1.205 (m, 6H). ^{13}C NMR (100 MHz, $CDCl_3$) δ 136.57, 135.08, 129.72, 127.61, 49.82, 32.70, 26.13, 25.71, 21.14. MS-APCI *m/z*: 239.0 $[M + H]^+$. HPLC analysis: Rt = 12.19 min, purity 95.09%, 80:20 CH_3OH/H_2O.

4-[2-(1-Methylpropyldisulfanyl)] phenol (43). Yield: 74.8%; ^{1}H NMR (400 MHz, $CDCl_3$) δ 7.421 (d, J = 8.4 Hz, 2H), 7.137 (d, 8.0 Hz, 2H), 3.676 (s, 3H), 2.954 (t, J = 7.2 Hz, 2H), 2.736 (t, J = 7.2 Hz, 2H), 2.337 (s, 3H). ^{13}C NMR (100 MHz, $CDCl_3$) δ 137.47, 133.49, 129.93, 128.69, 51.97, 33.62, 33.06, 21.16. MS-APCI *m/z*: 243.0 $[M + H]^+$. HPLC analysis: Rt = 7.89 min, purity 98.74%, 85:15 CH_3OH/H_2O.

4-[2-(Isopropyldisulfanyl)] phenol (44). Yield: 65.9%; ^{1}H NMR (400 MHz, $CDCl_3$) δ 7.441 (d, J = 8.4 Hz, 1H), 7.378 (d, J = 8.0 Hz, 1H), 7.149 (d, J = 8.0 Hz, 1H), 7.103 (d, J = 8.0 Hz, 1H), 3.769 (s, 1H), 3.604 (s, 3H), 3.488 (s, 1H), 2.340 (s, 3H). ^{13}C NMR (100 MHz, $CDCl_3$) δ 169.55, 138.05, 133.88, 129.72, 128.52, 52.49, 40.55, 21.14. MS-APCI *m/z*: 229.0 $[M + H]^+$. HPLC analysis: Rt = 10.54 min, purity 98.89%, 85:15 CH_3OH/H_2O.

3-[2-(4-Chlorophenyldisulfanyl)] propionic acid (45). Yield: 75.2%; ^{1}H NMR (400 MHz, $CDCl_3$) δ 7.465 (d, J = 8.4 Hz, 2H), 7.300 (d, J = 8.4 Hz, 2H), 2.57 (t, J = 7.0 Hz, 2H), 2.782 (t, J = 7.0 Hz, 2H). ^{13}C NMR (100 MHz, DMSO-d_6) δ 172.66, 135.63, 131.95, 129.32, 128.87, 33.45, 33.10. MS-ESI *m/z*: 49.3 [2 M−H]$^-$. HPLC analysis: Rt = 6.24 min, purity 99.01%, 85:15 CH_3OH/H_2O.

2-[2-(4-Chlorophenyldisulfanyl)] methyl acetate (46). Yield: 63.7%; ^{1}H NMR (400 MHz, $CDCl_3$) δ 7.482 (d, J = 8.8 Hz, 2H), 7.310 (d, J = 8.4 Hz, 2H), 3.604 (s, 3H), 3.492 (s, 2H). ^{13}C NMR (100 MHz, $CDCl_3$) δ 169.27, 134.70, 133.62, 130.01, 129.23, 52.55, 40.56. MS-APCI *m/z*: 246.0 [M−2H]$^-$. HPLC analysis: Rt = 3.82 min, purity 98.31%, 90:10 CH_3OH/H_2O.

4-Chlorophenyl 2-pyridyl disulfide (47). Yield: 77.7%; ^{1}H NMR (400 MHz, $CDCl_3$) δ 8.484 (d, J = 4.4 Hz, 1H), 7.650–7.588 (m, 2H), 7.458 (d, J = 8.4 Hz, 2H), 7.260 (s, 2H), 7.116 (t, J = 5.4 Hz, 1H). ^{13}C NMR (100 MHz, DMSO-d_6) δ 157.59, 149.71, 137.96, 134.41, 132.40, 129.26, 128.91, 121.63, 119.33. MS-APCI *m/z*: 254.0 $[M + H]^+$. HPLC analysis: Rt = 9.77 min, purity 99.26%, 85:15 CH_3OH/H_2O.

3-[2-(4-Chlorophenyldisulfanyl)] methyl propionate (48). Yield: 82.7%; ^{1}H NMR (400 MHz, $CDCl_3$) δ 7.460 (d, J = 8.8 Hz, 2H), 7.297 (d, J = 8.8 Hz, 2H), 3.678 (s, 3H), 2.960 (t, J = 7.2 Hz, 2H), 2.720 (t, J = 7.2 Hz, 2H). ^{13}C NMR (100 MHz, $CDCl_3$) δ 171.92, 135.56, 133.00, 129.18, 128.98, 51.94, 33.50, 33.16. MS-APCI *m/z*: 261.0 [M−H]$^-$. HPLC analysis: Rt = 9.31 min, purity 98.89%, 85:15 CH_3OH/H_2O.

2-[2-(Propionyloxydisulfanyl)] benzoic acid (49). Yield: 85.1%; ^{1}H NMR (400 MHz, DMSO-d_6) δ 8.100 (d, J = 7.6 Hz, 1H), 7.972 (d, J =

6.4 Hz, 1H), 7.677 (t, $J = 7.0$ Hz, 1H), 7.341 (t, $J = 7.4$ Hz, 1H), 2.872 (t, $J = 6.2$ Hz, 2H), 2.594 (t, $J = 8$ Hz, 2H). ^{13}C NMR (100 MHz, DMSO-d_6) δ 172.78, 167.68, 133.18, 131.68, 127.75, 125.71, 33.41, 32.66. MS-ESI m/z: 257.2 [M−H]$^-$. HPLC analysis: Rt = 7.85 min, purity 95.64%, 85:15 CH_3OH/H_2O.

2-[2-(Isopropyldisulfanyl)] benzoic acid (50). Yield: 78.7%; ^{1}H NMR (400 MHz, DMSO-d_6) δ 8.110 (d, $J = 7.2$ Hz, 1H), 7.947 (d, $J = 6.0$ Hz, 1H), 7.654 (t, $J = 7.0$ Hz, 1H), 7.315 (t, $J = 7.0$ Hz, 1H), 3.124–3.024 (m, 1H), 1.252 (d, $J = 6.8$ Hz, 6H). ^{13}C NMR (100 MHz, DMSO-d_6) δ 167.56, 141.16, 132.88, 131.41, 127.69, 125.50, 40.57, 22.32. MS-ESI m/z: 227.7 [M−H]$^-$. HPLC analysis: Rt = 6.46 min, purity 96.17%, 85:15 CH_3OH/H_2O.

2-Pyridyl *tert*-butyl disulfide (51). Yield: 69.3%; ^{1}H NMR (400 MHz, $CDCl_3$) δ 8.430 (d, $J = 4.0$ Hz, 1H), 7.795 (d, $J = 8.4$ Hz, 1H), 7.620 (t, $J = 6.8$ Hz, 1H), 7.053 (t, $J = 6.2$ Hz, 1H), 1.335 (s, 9H). ^{13}C NMR (100 MHz, $CDCl_3$) δ 161.57, 149.12, 136.90, 120.41, 119.59, 49.30, 29.76. MS-APCI m/z: 200.0 [M + H]$^+$. HPLC analysis: Rt = 6.89 min, purity 95.01%, 85:15 CH_3OH/H_2O.

2-Pyridyl 1-methylpropyl disulfide (52). Yield: 78.4%; ^{1}H NMR (400 MHz, $CDCl_3$) δ 8.443 (d, $J = 4.0$ Hz, 1H), 7.773 (d, $J = 8.4$ Hz, 1H), 7.659–7.636 (m, 1H), 7.082–7.054 (m, 1H), 2.937–2.853 (m, 1H), 1.780–1.692 (m, 1H), 1.588–1.535 (m, 1H), 1.307 (d, $J = 6.8$ Hz, 3H), 0.986 (t, $J = 4.0$ Hz, 3H). ^{13}C NMR (100 MHz, $CDCl_3$) δ 161.30, 149.28, 37.11, 20.54, 119.67, 48.54, 28.86, 19.89, 11.55. MS-APCI m/z: 200.0 [M + H]$^+$. HPLC analysis: Rt = 6.06 min, purity 98.83%, 85:15 CH_3OH/H_2O.

2-[2-(1-Methylpropyldisulfanyl)] aniline (53). Yield: 68.3%; ^{1}H NMR (400 MHz, $CDCl_3$) δ 7.457–7.435 (m, 1H), 7.156–7.114 (m, 1H), 6.739–6.663 (m, 2H), 2.896–2.812 (m, 1H), 1.801–1.696 (m, 1H), 1.589–1.481 (m, 1H), 1.301 (d, $J = 6.8$ Hz, 3H), 0.908 (t, $J = 7.2$ Hz, 3H). ^{13}C NMR (100 MHz, $CDCl_3$) δ 147.76, 34.88, 130.62, 119.74, 118.39, 115.65, 47.74, 28.67, 19.80, 1.37. MS-ESI m/z: 213.9 [M + H]$^+$. HPLC analysis: Rt = 3.18 min, purity 96.07%, 90:10 CH_3OH/H_2O.

2-(Cyclohexyldisulfanyl) benzo[*d*] oxazole (54). Yield: 81.3%; ^{1}H NMR (400 MHz, $CDCl_3$) δ 7.672 (d, $J = 8.4$ Hz, 1H), 7.494 (t, $J = 8.4$ Hz, 1H), 7.306 (t, $J = 4.0$ Hz, 2H), 3.111–3.057 (m, 1H), 2.110 (d, $J = 10.0$ Hz, 2H), 1.605 (d, $J = 10.0$ Hz, 2H), 1.471–1.251 (m, 6H). ^{13}C NMR (100 MHz, $CDCl_3$) δ 164.01, 152.33, 142.04, 124.61, 124.54, 119.32, 110.23, 49.96, 32.27, 25.92, 25.44. MS-APCI m/z: 267.0 [M + H]$^+$. HPLC analysis: Rt = 8.90 min, purity 95.12%, 80:20 CH_3OH/H_2O.

2-(Isopropyldisulfanyl) benzo[*d*] oxazole (55). Yield: 71.3%; ^{1}H NMR (400 MHz, $CDCl_3$) δ 7.670 (d, $J = 8.4$ Hz, 1H), 7.497 (d, $J = 8.8$ Hz, 1H), 7.321–7.293 (m, 2H), 3.414–3.313 (m, 1H), 1.402 (d, $J = 6.8$ Hz, 6H). ^{13}C NMR (100 MHz, $CDCl_3$) δ 162.88, 152.06, 141.81, 125.63, 125.31, 119.54, 110.99, 41.96, 22.28. MS-APCI m/z: 226.0 [M + H]$^+$. HPLC analysis: Rt = 10.63 min, purity 97.36%, 80:20 CH_3OH/H_2O.

2-(*tert*-Butyldisulfanyl) benzo[*d*] oxazole (56). Yield: 58.6%; ^{1}H NMR (400 MHz, DMSO-d_6) δ 7.746–7.697 (m, 2H), 7.407–7.379 (m, 2H), 1.371 (s, 9H). ^{13}C NMR (100 MHz, DMSO-d_6) δ 162.76, 151.96, 141.84, 125.60, 125.28, 119.52, 110.94, 49.86, 29.50. MS-APCI m/z: 240.0 [M + H]$^+$. HPLC analysis: Rt = 12.20 min, purity 98.05%, 80:20 CH_3OH/H_2O.

2-(Cyclopentyldisulfanyl) benzo[*d*] oxazole (57). Yield: 74.5%; ^{1}H NMR (400 MHz, $CDCl_3$) δ 7.689–7.665 (m, 1H), 7.511–7.487 (m, 1H), 7.322–7.293 (m, 2H), 3.672–3.641 (m, 1H), 2.081–2.018 (m, 2H), 1.810–1.741 (m, 4H), 1.654–1.617 (m, 2H). ^{13}C NMR (100 MHz, $CDCl_3$) δ 163.88, 152.39, 142.03, 124.65, 124.57, 119.34, 110.24, 50.60, 32.76, 24.77. MS-APCI m/z: 252.0 [M + H]$^+$. HPLC analysis: Rt = 8.13 min, purity 98.99%, 80:20 CH_3OH/H_2O.

2-(Isopropyldisulfanyl)-1H-benzo[*d*] imidazole (58). Yield: 69.7%; ^{1}H NMR (400 MHz, DMSO-d_6) δ 7.501 (d, $J = 2.4$ Hz, 2H), 7.123 (d, $J = 4.0$ Hz, 2H), 3.370–3.269 (m, 1H), 1.286 (d, $J = 6.8$ Hz, 6H). ^{13}C NMR (100 MHz, DMSO-d_6) δ 149.42, 132.29, 122.36, 109.52, 41.41, 21.9. MS-ESI m/z: 224.9 [M + H]$^+$. HPLC analysis: Rt = 9.60 min, purity 98.94%, 80:20 CH_3OH/H_2O.

2-(Cyclohexyldisulfanyl)-1H-benzo[*d*] imidazole (59). Yield: 75.4%; ^{1}H NMR (400 MHz, DMSO-d_6) δ 7.491 (d, $J = 3.6$ Hz, 2H), 7.172 (d, $J = 9.2$ Hz, 2H), 1.988 (d, $J = 11.2$ Hz, 1H), 1.715–1.684 (m, 2H), 1.402–1.166 (m, 8H). ^{13}C NMR (100 MHz, DMSO-d_6) δ 168.13, 132.28, 122.35, 109.51, 49.16, 31.78, 25.32. MS-ESI m/z: 265.3 [M + H]$^+$. HPLC analysis: Rt = 7.18 min, purity 97.86%, 80:20 CH_3OH/H_2O.

2-(Cyclopentyldisulfanyl)-1H-benzo[*d*] imidazole (60). Yield: 77.3%; ^{1}H NMR (400 MHz, DMSO-d_6) δ 12.787 (s, 1H), 7.504 (s, 2H), 7.185 (d, $J = 2.8$ Hz, 2H), 2.004–1.966 (m, 1H), 1.691–1.594 (m, 8H). ^{13}C NMR (100 MHz, DMSO-d_6) δ 149.22, 132.29, 122.15, 109.51, 50.06, 32.19, 24.31. MS-APCI m/z: 251.0 [M + H]$^+$. HPLC analysis: Rt = 6.09 min, purity 98.34%, 80:20 CH_3OH/H_2O.

2-(*tert*-Butyldisulfanyl)-1H-benzo[*d*] imidazole (61). Yield: 83.2%; ^{1}H NMR (400 MHz, DMSO-d_6) δ 12.493 (s, 1H), 7.124 (d, $J = 2.4$ Hz, 4H), 1.326 (s, 9H). ^{13}C NMR (100 MHz, DMSO-d_6) δ 149.74, 132.30, 122.40, 109.56, 49.27, 29.12. MS-ESI m/z: 238.9 [M + H]$^+$. HPLC analysis: Rt = 11.62 min, purity 97.58%, 80:20 CH_3OH/H_2O.

2-(Propyldisulfanyl)-1H-benzo[*d*] imidazole (62). Yield: 81.7%; ^{1}H NMR (400 MHz, $CDCl_3$) δ 7.553 (s, 2H), 7.250–7.225 (m, 2H), 2.857 (t, $J = 7.2$ Hz, 2H), 1.805–1.713 (m, 2H), 0.995 (t, $J = 7.4$ Hz, 3H). ^{13}C NMR (100 MHz, DMSO-d_6) δ 123.07, 122.19, 118.77, 111.62, 41.00, 21.97, 13.10. MS-ESI m/z: 224.9 [M + H]$^+$. HPLC analysis: Rt = 6.01 min, purity 96.21%, 80:20 CH_3OH/H_2O.

2-(1-Methylpropyldisulfanyl)-1H-benzo[*d*] imidazole (63). Yield: 75.9%; ^{1}H NMR (400 MHz, $CDCl_3$) δ 7.544 (s, 2H), 7.249–7.226 (m, 2H), 3.019–2.934 (m, 1H), 1.815–1.709 (m, 1H), 1.621–1.513 (m, 1H), 1.325 (d, $J = 6.8$ Hz, 3H), 0.969 (t, $J = 7.4$ Hz, 3H). ^{13}C NMR (100 MHz, $CDCl_3$) δ 150.81, 139.48, 122.74, 114.75, 49.04, 28.71, 19.66, 11.48. MS-ESI m/z: 238.9 [M + H]$^+$. HPLC analysis: Rt = 9.60 min, purity 97.21%, 80:20 CH_3OH/H_2O.

2-(*tert*-Butyldisulfanyl)-5-(difluoromethoxy)-1H-benzo[*d*] imidazole (64). Yield: 81.7%; ^{1}H NMR (400 MHz, $CDCl_3$) δ 7.481 (d, $J = 8.0$ Hz, 1H), 7.321 (s, 1H), 7.042 (d, $J = 8.8$ Hz, 1H), 6.500 (t, $J = 74.0$ Hz, 1H), 1.373 (s, 9H). ^{13}C NMR (100 MHz, $CDCl_3$) δ 152.59, 146.92, 118.97, 116.39, 115.70, 113.81, 49.88, 29.50. MS-APCI m/z: 305.0 [M + H]$^+$. HPLC analysis: Rt = 7.46 min, purity 94.15%, 80:20 CH_3OH/H_2O.

2-(1-Methylpropyldisulfanyl)-5-(difluoromethoxy)-1H-benzo[*d*] imidazole (65). Yield: 80.2%; ^{1}H NMR (400 MHz, $CDCl_3$) δ 7.495 (d, $J = 8.8$ Hz, 1H), 7.331 (s, 1H), 7.052 (d, $J = 7.2$ Hz, 1H), 6.507 (t, $J = 74.0$ Hz, 1H), 3.029–2.945 (m, 1H), 1.818–1.712 (m, 1H), 1.632–1.524 (m, 1H), 1.333 (d, $J = 6.4$ Hz, 3H), 0.980 (t, $J = 7.2$ Hz, 3H). ^{13}C NMR (100 MHz, DMSO-d_6) δ 151.34, 146.91, 119.90, 117.34, 115.18, 114.78, 48.46, 28.42, 19.78, 11.48. MS-APCI m/z: 303.0 [M−H]$^-$. HPLC analysis: Rt = 5.96 min, purity 96.68%, 80:20 CH_3OH/H_2O.

2-(Propyldisulfanyl)-5-nitro-1H-benzo[*d*] imidazole (66). Yield: 89.1%; ^{1}H NMR (400 MHz, $CDCl_3$) δ 8.475 (s, 1H), 8.204 (d, $J = 6.8$ Hz, 1H), 7.597 (d, $J = 8.8$ Hz, 1H), 2.897 (t, $J = 7.2$ Hz, 2H), 1.821–1.730 (m, 2H), 1.019 (t, $J = 7.2$ Hz, 3H). ^{13}C NMR (100 MHz, $CDCl_3$) δ 143.04, 137.83, 132.70, 119.39, 118.37, 109.69, 105.09, 40.96, 21.99, 13.06. MS-APCI m/z: 270.0 [M + H]$^+$. HPLC analysis: Rt = 9.60 min, purity 98.94%, 80:20 CH_3OH/H_2O.

2-(Cyclopentyldisulfanyl)-5-nitro-1H-benzo[*d*] imidazole (67). Yield: 79.1%; ^{1}H NMR (400 MHz, $CDCl_3$) δ 8.473 (s, 1H), 8.193 (d, $J = 6.8$ Hz, 1H), 7.595 (d, $J = 8.8$ Hz, 1H), 3.501–3.471 (m, 1H), 1.784–1.630 (m, 8H). ^{13}C NMR (100 MHz, $CDCl_3$) δ 156.37, 143.60, 118.81, 51.08, 32.85, 24.73. MS-APCI m/z: 294.0 [M−H]$^-$. HPLC analysis: Rt = 7.44 min, purity 96.10%, 80:20 CH_3OH/H_2O.

2-(*tert*-Butyldisulfanyl)-5-nitro-1H-benzo[*d*] imidazole (68). Yield: 85.2%; ^{1}H NMR (400 MHz, $CDCl_3$) δ 8.468 (s, 1H), 1.191 (d, $J = 6.8$ Hz, 1H), 7.587 (d, $J = 8.8$ Hz, 1H), 1.398 (s, 9H). ^{13}C NMR (100 MHz, $CDCl_3$) δ 143.66, 118.86, 50.43, 29.63. MS-ESI m/z: 284.2 [M + H]$^+$. HPLC analysis: Rt = 9.60 min, purity 99.09%, 80:20 CH_3OH/H_2O.

2-(1-Methylpropyldisulfanyl)-5-nitro-1H-benzo[*d*] imidazole (69). Yield: 76.3%; ^{1}H NMR (400 MHz, $CDCl_3$) δ 8.469, (s, 1H), 8.192 (d, $J = 6.4$ Hz, 1H), 7.590 (d, $J = 8.8$ Hz, 1H), 3.071–2.987 (m, 1H), 1.809–1.740 (m, 1H), 1.633–1.561(m, 1H), 1.350 (d, $J = 6.8$ Hz, 3H),

0.996 (t, $J = 7.2$ Hz, 3H). ^{13}C NMR (100 MHz, $CDCl_3$) δ 156.63, 143.59, 118.82, 49.31, 28.74, 19.63, 11.45. MS-APCI *m/z*: 282.0 $[M-H]^-$. HPLC analysis: Rt = 6.61 min, purity 97.93%, 80:20 CH_3OH/H_2O.

2-(*tert*-Butyldisulfanyl)-5-methoxy-1H-benzo [*d*] imidazole (70). Yield: 65.7%; ^{1}H NMR (400 MHz, $CDCl_3$) δ 7420 (d, $J = 8.4$ Hz, 1H), 7.019 (s, 1H), 6.858 (d, $J = 8.8$ Hz, 1H), 3.819 (s, 3H), 1.346 (s, 9H). ^{13}C NMR (100 MHz, DMSO-d_6) δ 156.25, 148.73, 112.03, 55.87, 49.47, 29.58. MS-APCI *m/z*: 269.0 $[M + H]^+$. HPLC analysis: Rt = 5.15 min, purity 98.45%, 80:20 CH_3OH/H_2O.

2-(Propyldisulfanyl)-5-methoxy-1H-benzo [*d*] imidazole (71). Yield: 75.8%; ^{1}H NMR (400 MHz, $CDCl_3$) δ 7.457 (d, $J = 8.8$ Hz, 1H), 7.046 (d, $J = 3.6$ Hz, 1H), 6.893 (d, $J = 8.8$ Hz, 1H), 3.838 (s, 3H), 2.841 (t, $J = 7.2$ Hz, 2H), 1.771–1.682 (m, 2H), 0.964 (t, $J = 7.2$ Hz, 3H). ^{13}C NMR (100 MHz, $CDCl_3$) δ 158.64, 140.29, 132.05, 125.20, 116.73, 115.76, 96.96, 56.35, 53.88, 18.77, 13.79. MS-APCI *m/z*: 255.0 $[M + H]^+$. HPLC analysis: Rt = 3.40 min, purity 95.79%, 80:20 CH_3OH/H_2O.

2-(1-Methylpropyldisulfanyl)-5-methoxy-1H-benzo [*d*] imidazole (72). Yield: 77.7%; ^{1}H NMR (400 MHz, $CDCl_3$) δ 7.432 (d, $J = 8.8$ Hz, 1H), 7.025 (s, 1H), 6.875 (d, $J = 8.8$ Hz, 1H), 3.389 (s, 3H), 3.015–2.931 (m, 1H), 1.810–1.704 (s, 1H), 1.619–1.511 (m, 1H), 1.321 (d, $J = 6.8$ Hz, 3H), 0.959 (t, $J = 7.6$ Hz, 3H). ^{13}C NMR (100 MHz, $CDCl_3$) δ 156.34, 148.31, 112.26, 97.37, 55.88, 48.40, 28.41, 19.87, 11.49. MS-APCI *m/z*: 269.0 $[M + H]^+$. HPLC analysis: Rt = 3.53 min, purity 94.10%, 80:20 CH_3OH/H_2O.

4.4. Screening of disulfides against Trx by NBL-SS

The *E.coli* Trx was reduced with excessive DTT, and then the excess DTT was removed by a Sephadex G-25 desalting column. The concentration of the *E.coli* Trx was quantified by a Microplate Reader using the Bradford asaay. The reduced Trx (10 μM) was incubated with different concentrations (100 μM, 20 μM, 10 μM) of compounds in TE buffer (pH = 7.4) at 37 °C in 96-well plates for 30 min. The positive control group only had reduced Trx and TE buffer but without tested compounds. To eliminate the interference of DMSO, we set a blank control group where the same amount DMSO was introduced. Then, the probe NBL-SS (5 μM) was added into all wells quickly and incubated for another 5 min, and the fluorescence intensity was monitored with a Microplate Reader (λ_{ex} = 610 nm; λ_{em} = 661 nm, FlexStation 3, USA).

4.5. Determination of fluorescence of Trx redox status

We determined the fluorescence intensity of Trx redox status at 340 nm after excitation at 280 nm. First, the fluorescence intensity of the reduced Trx was measured in TE buffer at 25 °C, then the reduced Trx and the **68** were incubated together, and the fluorescence intensity of Trx was measured every minute in TE buffer at 25 °C for 30 min. The **68** was dissolved in DMSO, the reduced Trx was prepared by DTT. All the data were determined by a Cary Eclipse Fluorescence spectrophotometer (Agilent Technologies).

4.6. Kinetic studies [31,35,39,51]

The reactions of compound **68, 69** (10 μM each) with Trx (<10 μM) in TE buffer (pH = 7.4, containing 1‰ DMSO) were monitored by measuring the fluorescence intensity at 340 nm after excitation at 280 nm. The reactions were carried out at 25 °C. The reduced Trx was prepared by DTT. The second-order rate constants for the reactions were determined by fitting the fluorescence intensities of the sample to the second-order equation (1):

$$\frac{1}{[A]_0 - [B]_0} \ln\left(\frac{[B]_0[A]}{[A]_0[B]}\right) = k^{\cdot} t \quad (1)$$

where $[A]_0$ and $[B]_0$ were the initial concentrations of Trx and compounds, respectively. $\ln\ln([B]_0[A]/[A]_0[B])$, $[A]$ and $[B]$ were $[A]_0-[A]_0(F_{re}-F_t)/(F_{re}-F_{ox})$ and $[B]_0-[A]_0(F_{re}-F_t)/(F_{re}-F_{ox})$ at a given time, respectively. These results were shown in Fig. S2 & **Tables S1/2**.

4.7. Determination of Trx redox states by probe Naph-EA-mal [43]

The stock Trx was incubated with DTT to prepare the reduced Trx. The triploid volume of cold-acetone (acetone was put at −20 °C for a 3–5 h) was added to precipitate the protein for 1 h at −80 °C, and the reaction mixture was centrifuged at 4 °C and removed supernatant. Then PBS and SDS were added to thaw Trx and the Trx were incubated with **68** for 30 min, the probe Naph-EA-mal (10 mM) which is a thiol probe for protein labeling and bioimaging was added, incubated, and shaken every 15 min. After an hour, cold-acetone was added to precipitate the protein for 1 h at −80 °C, the reaction mixture was centrifuged at 4 °C and the supernatant was removed. PBS with SDS (1%, w/v) were added to dissolve the protein, and all samples were boiled with loading buffer and then were analyzed by SDS-PAGE. The gel images were acquired with a Gel imager (G: BOX Chemi XX9, UK) and stained with CB.

4.8. Cell cultures

The cell culture conditions were described in previous publications [52,53].

4.9. Cytotoxicity assays

4.9.1. MTT assay [52,53]

HeLa cells (1×10^4 cells/well) were incubated with compounds **4, 5, 6, 19, 22, 24, 68** and **69** in triplicate in a 96-well plate for the indicated time at 37 °C in a final volume of 100 μL. Cells were treated only with DMSO as a control group. At the end of the treatment with eight compounds (48 h and 72 h), 10 μL of MTT (5 mg/mL) was added to each well and continued incubated for 4 h at 37 °C. An extraction buffer (100 μL, 10% SDS, 5% isobutanol, 0.1% HCl) was added, and the cells were incubated overnight at 37 °C. The absorbance was measured at 570 nm on Multiskan GO (Thermo Scientific)

4.9.2. Trypan blue exclusion assay [52,53]

HeLa cells were seeded in 12-well plates and treated with different concentrations of **68** for 72 h. Cells were treated with DMSO only as a control, and cell viability was determined by the trypan blue exclusion assay. After treatment, the cells were stained with trypan blue (0.4%, w/v), and the number of viable (non-stained) and dead (stained) cells were counted by a microscope.

4.10. Imaging Trx activity in HeLa cells by NBL-SS

The cells were seeded in 12-well plates (2×10^4 cells/well) for 24 h at 37 °C, and then, the cells were treated with indicated concentrations of **68** (10 μM) for 6 h, 12 h, 24 h at 37 °C, respectively. Then NBL-SS (5 μM) in DMSO was added and continued incubated for another 5 min at 37 °C in the dark. After washing the cells with PBS twice to remove the remaining NBL-SS, the fluorescence images were acquired with a Floid cell imaging station (Life Technology).

4.11. Determination of intracellular ROS

HeLa cells were incubated with different concentrations of **68** in 12-well plates (1×10^4 cells/well) for 48 h, while the cells incubated only with DMSO served as a control. After removing the medium, the cells were continued to incubate with 2′, 7′-dichlorofluorescein diacetate (DCFH-DA, 10 μM) or DHE (10 μM) in a fresh medium for 0.5 h in the dark. Following incubation, the cell images were observed by a fluorescence microscope.

4.12. PAO-Sepharose assay

This assay was based on the binding of vicinal dithiols to phenylarsine oxide (PAO). PAO beads (PAO-Sepharose) was prerpared by our group [44,46]. Reduced Trx was captured by PAO and hence pulled down, while oxidized forms remained in the supernatant. HeLa cells were treated with **68** (40 μM) for 48 h. Total cellular proteins were extracted by RIPA buffer and quantified by the Bradford method. Samples were loaded to PAOsepharose and incubated at room temperature for 30 min on a rotating shaker. The supernatant (containing oxidized Trx) was collected and the sepharose (containing reduced Trx) was washed with TE buffer. Reduced Trx was then knocked out by DMPS (20 mM) in TE buffer. All samples were separated by 15% SDS-PAGE under reducing conditions with the presence of 100 mM DTT in loading buffer and electroblotted onto PVDF membrane for Western blot analysis.

4.13. Western blotting

HeLa cells were treated with **68** (40 μM) in 100 mm dishes (2×10^6 cells/dish) for 48 h, while the control group was incubated only with DMSO. The cells were lysed with RIPA buffer and protein concentration was quantified using the Bradford procedure. Cell lysates were separated by SDS-PAGE and electroblotted onto PVDF membranes (Millipore, USA). After blocking in TBST 20 mM Tris-HCl, pH 7.6, 0.14 mM NaCl, and 0.1% Tween-20) with 5% non-fat milk at room temperature for 2 h, the membranes were incubated with primary antibody overnight at 4 °C. Under reducing conditions, equal amounts of protein in each lysate sample were separated by SDS-PAGE (12% gel, 40 mg per lane) and then transferred to poly-vinylidene fluoride (PVDF) membrane (Millipore, USA). The blots were blocked in TBST with 5% non-fat milk for 2 h at room temperature, then, membranes were incubated overnight at 4 °C with the specific primary antibody in 5% non-fat milk. The membranes were washed three times by TBST and were incubated with the peroxidase-conjugated secondary antibodies at room temperature for 1 h. The signal was detected using an enhanced chemiluminescence (ECL) kit from Vazyme Biotech (Nanjing, China).

4.14. Apoptosis assays

4.14.1. Determination of caspase-3 activity

We treated HeLa cells with different concentrations of **68** for 48 h, then collected the cells and lysed them with RIPA buffer. Protein content was quantified by the Bradford method and the activity of caspase-3 was determined as described [45,54].

4.14.2. Annexin V/PI staining

HeLa cells (1×10^6 cells/dish) were incubated in 6-well plates with different concentrations of **68** for 48 h. Then cells were collected and washed twice with PBS. Apoptotic, necrotic and live cells were identified by the PI double and Annexin V-FITC staining assay according to the manufacturer's instructions. Finally, the data were determined by a FACSCanto™ flow cytometer (BD Biosciences, USA), and were analyzed with the CellQuest software.

Declaration of Competing Interest

The authors declare that they have no known competing financial interests or personal relationships that could have appeared to influence the work reported in this paper.

Acknowledgments

Financial supports from the National Natural Science Foundation of China (22077055, 21778028 and 82003779), the Natural Science Foundation of Gansu Province (20JR5RA311 & 18JR4RA003), and the 111 project are acknowledged.

Appendix A. Supplementary material

Supplementary data to this article can be found online at https://doi.org/10.1016/j.bioorg.2021.104814.

References

[1] M.R. Atashzar, R. Baharlou, J. Karami, H. Abdollahi, R. Rezaei, F. Pourramezan, S. H. Zoljalali Moghaddam, Cancer stem cells: A review from origin to therapeutic implications, J. Cell Physiol. 235 (2) (2020) 790–803.
[2] G. Bocci, R.S. Kerbel, Pharmacokinetics of metronomic chemotherapy: a neglected but crucial aspect, Nat. Rev. Clin. Oncol. 13 (11) (2016) 659–673.
[3] J. Liao, Y. Jia, Y. Wu, K. Shi, D. Yang, P. Li, Z. Qian, Physical-, chemical-, and biological-responsive nanomedicine for cancer therapy, Wiley Interdiscip. Rev. Nanomed. Nanobiotechnol. 12 (1) (2020), https://doi.org/10.1002/wnan.1581.
[4] Y. Meyer, B.B. Buchanan, F. Vignols, J.-P. Reichheld, Thioredoxins and glutaredoxins: unifying elements in redox biology, Annu. Rev. Genet. 43 (1) (2009) 335–367.
[5] A. Holmgren, Thioredoxin, Annu. Rev. Biochem. 54 (1) (1985) 237–271.
[6] M. Bian, R. Fan, S. Zhao, W. Liu, Targeting the thioredoxin system as a strategy for cancer therapy, J. Med. Chem. 62 (16) (2019) 7309–7321.
[7] K.F. Tonissen, G. Di Trapani, Thioredoxin system inhibitors as mediators of apoptosis for cancer therapy, Mol. Nutr. Food Res. 53 (1) (2009) 87–103.
[8] J. Lu, A. Holmgren, The thioredoxin antioxidant system, Free Radic. Biol. Med. 66 (2014) 75–87.
[9] F. Mohammadi, A. Soltani, A. Ghahremanloo, H. Javid, S.I. Hashemy, The thioredoxin system and cancer therapy: a review, Cancer Chemoth. Pharm. 84 (5) (2019) 925–935.
[10] J.J. Jia, W.S. Geng, Z.Q. Wang, L. Chen, X.S. Zeng, The role of thioredoxin system in cancer: strategy for cancer therapy, Cancer Chemoth. Pharm. 84 (3) (2019) 453–470.
[11] N. Wakasugi, Y. Tagaya, H. Wakasugi, A. Mitsui, M. Maeda, J. Yodoi, T. Tursz, Adult T-cell leukemia-derived factor thioredoxin, produced by both human T-lymphotropic virus Type-I and epstein-barr virus-transformed lymphocytes, acts as an autocrine growth-factor and synergizes with interleukin-1 and interleukin-2, Proc. Natl. Acad. Sci. USA 87 (21) (1990) 8282–8286.
[12] D. Hedley, M. Pintilie, J. Woo, T. Nicklee, A. Morrison, D. Birle, A. Fyles, M. Milosevic, R. Hill, Up-regulation of the redox mediators thioredoxin and apurinic/apyrimidinic excision (APE)/ref-1 in hypoxic microregions of invasive cervical carcinomas, mapped using multispectral, wide-field fluorescence image analysis, Am. J. Pathol. 164 (2) (2004) 557–565.
[13] G.J. Samaranayake, C.I. Troccoli, M. Huynh, R.D.Z. Lyles, K. Kage, A. Win, V. Lakshmanan, D. Kwon, Y. Ban, S.X. Chen, E.R. Zarco, M. Jorda, K.L. Burnstein, P. Rai, Thioredoxin-1 protects against androgen receptor-induced redox vulnerability in castration-resistant prostate cancer, Nat. Commun. 8 (1) (2017), https://doi.org/10.1038/s41467-017-01269-x.
[14] M. Bhatia, K.L. McGrath, G. Di Trapani, P. Charoentong, F. Shah, M.M. King, F. M. Clarke, K.F. Tonissen, The thioredoxin system in breast cancer cell invasion and migration, Redox. Biol. 8 (2016) 68–78.
[15] F. Lin, P. Zhang, Z. Zuo, F. Wang, R. Bi, W. Shang, A. Wu, J.u. Ye, S. Li, X. Sun, J. Wu, L. Jiang, Thioredoxin-1 promotes colorectal cancer invasion and metastasis through crosstalk with S100P, Cancer Lett. 401 (2017) 1–10.
[16] H.Y. Han, D.J. Bearss, L.W. Browne, R. Calaluce, R.B. Nagle, D.D. Von Hoff, Identification of differentially expressed genes in pancreatic cancer cells using cDNA microarray, Cancer Res. 62 (10) (2002) 2890–2896.
[17] R. Fan, M.L. Bian, L.H. Hu, W.K. Liu, A new rhodium(I) NHC complex inhibits TrxR: In vitro cytotoxicity and in vivo hepatocellular carcinoma suppression, Eur. J. Med. Chem. 183 (2019).
[18] S. Banerjee, S. Mukherjee, S. Mitra, P. Singhal, Altered expression of mitochondrial antioxidants in oral squamous cell carcinoma, J. Oral. Sci. 59 (3) (2017) 439–446.
[19] T.M. Grogan, C. Fenoglio-Prieser, R. Zeheb, W. Bellamy, Y. Frutiger, E. Vela, G. Stemmerman, J. Macdonald, L. Richter, A. Gallegos, G. Powis, Thioredoxin, a putative oncogene product, is overexpressed in gastric carcinoma and associated with increased proliferation and increased cell survival, Hum. Pathol. 31 (4) (2000) 475–481.
[20] L.E. Shao, M.B. Diccianni, T. Tanaka, R. Gribi, A.L. Yu, J.D. Pullen, B.M. Camitta, J. Yu, Thioredoxin expression in primary T-cell acute lymphoblastic leukemia and its therapeutic implication, Cancer Res. 61 (19) (2001) 7333–7338.
[21] H.J. Kim, H.-Z. Chae, Y.-J. Kim, Y.H. Kim, T.-S. Hwang, E.-M. Park, Y.-M. Park, Preferential elevation of Prx I and Trx expression in lung cancer cells following hypoxia and in human lung cancer tissues, Cell Biol. Toxicol. 19 (5) (2003) 285–298.
[22] S.J. Welsh, W.T. Bellamy, M.M. Briehl, G. Powis, The redox protein thioredoxin-1 (Trx-1) increases hypoxia-inducible factor 1alpha protein expression: Trx-1 overexpression results in increased vascular endothelial growth factor production and enhanced tumor angiogenesis, Cancer Res. 62 (17) (2002) 5089–5095.
[23] J. Ceccarelli, L. Delfino, E. Zappia, P. Castellani, M. Borghi, S. Ferrini, F. Tosetti, A. Rubartelli, The redox state of the lung cancer microenvironment depends on the levels of thioredoxin expressed by tumor cells and affects tumor progression and response to prooxidants, Int. J. Cancer 123 (8) (2008) 1770–1778.
[24] L. Chaiswing, J.M. Bourdeau-Heller, W. Zhong, T.D. Oberley, Characterization of redox state of two human prostate carcinoma cell lines with different degrees of aggressiveness, Free Radic. Biol. Med. 43 (2) (2007) 202–215.

[25] S.J. Kim, Y. Miyoshi, T. Taguchi, Y. Tamaki, H. Nakamura, J. Yodoi, K. Kato, S. Noguchi, High thioredoxin expression is associated with resistance to docetaxel in primary breast cancer, Clin. Cancer Res. 11 (23) (2005) 8425–8430.
[26] G. Powis, D.L. Kirkpatrick, M. Angulo, A. Baker, Thioredoxin redox control of cell growth and death and the effects of inhibitors, Chem. Biol. Interact. 111-112 (1998) 23–34.
[27] D.F.D. Mahmood, A. Abderrazak, K. El Hadri, T. Simmet, M. Rouis, The thioredoxin system as a therapeutic target in human health and disease, Antioxid. Redox. Sign. 19 (11) (2013) 1266–1303.
[28] P. Gao, M. Shi, R. Wei, W. Pan, X. Liu, N.a. Li, B.o. Tang, A biomimetic MOF nanoreactor enables synergistic suppression of intracellular defense systems for augmented tumor ablation, Chem. Commun. (Camb) 56 (6) (2020) 924–927.
[29] W. Cai, L. Zhang, Y. Song, B. Wang, B. Zhang, X. Cui, G. Hu, Y. Liu, J. Wu, J. Fang, Small molecule inhibitors of mammalian thioredoxin reductase, Free Radic. Biol. Med. 52 (2) (2012) 257–265.
[30] J.M. Zhang, B.X. Zhang, X.M. Li, X. Han, R.J. Liu, J.G. Fang, Small molecule inhibitors of mammalian thioredoxin reductase as potential anticancer agents: An update, Med. Res. Rev. 39 (1) (2019) 5–39.
[31] T.R. DiRaimondo, N.M. Plugis, X.i. Jin, C. Khosla, Selective inhibition of extracellular thioredoxin by asymmetric disulfides, J. Med. Chem. 56 (3) (2013) 1301–1310.
[32] G. Powis, D.L. Kirkpatrick, Thioredoxin signaling as a target for cancer therapy, Curr. Opin. Pharm. 7 (4) (2007) 392–397.
[33] R.K. Ramanathan, D.L. Kirkpatrick, C.P. Belani, D. Friedland, S.B. Green, H.-H. Chow, C.A. Cordova, S.P. Stratton, E.R. Sharlow, A. Baker, T. Dragovich, A phase I pharmacokinetic and pharmacodynamic study of PX-12, a novel inhibitor of thioredoxin-1, in patients with advanced solid tumors, Clin. Cancer Res. 13 (7) (2007) 2109–2114.
[34] R.K. Ramanathan, J. Abbruzzese, T. Dragovich, L. Kirkpatrick, J.M. Guillen, A. F. Baker, L.A. Pestano, S. Green, D.D. Von Hoff, A randomized phase II study of PX-12, an inhibitor of thioredoxin in patients with advanced cancer of the pancreas following progression after a gemcitabine-containing combination, Cancer Chemoth. Pharm. 67 (3) (2011) 503–509.
[35] D.L. Kirkpatrick, M. Kuperus, M. Dowdeswell, N. Potier, L.J. Donald, M. Kunkel, M. Berggren, M. Angulo, G. Powis, Mechanisms of inhibition of the thioredoxin growth factor system by antitumor 2-imidazolyl disulfides, Biochem. Pharmacol. 55 (7) (1998) 987–994.
[36] J.R. Gasdaska, D.L. Kirkpatrick, W. Montfort, M. Kuperus, S.R. Hill, M. Berggren, G. Powis, Oxidative inactivation of thioredoxin as a cellular growth factor and protection by a Cys(73)->Ser mutation, Biochem. Pharmacol. 52 (11) (1996) 1741–1747.
[37] S.F. Sousa, R.P.P. Neves, S.O. Waheed, P.A. Fernandes, M.J. Ramos, Structural and mechanistic aspects of S-S bonds in the thioredoxin-like family of proteins, Biol. Chem. 400 (5) (2019) 575–587.
[38] G. Hu, H. Jia, L. Zhao, D.-H. Cho, J. Fang, Small molecule fluorescent probes of protein vicinal dithiols, Chin. Chem. Lett. 30 (10) (2019) 1704–1716.
[39] H. Jia, G. Hu, D. Shi, L.u. Gan, H. Zhang, X. Yao, J. Fang, Fluorophore-dependent cleavage of disulfide bond leading to a highly selective fluorescent probe of thioredoxin, Anal. Chem. 91 (13) (2019) 8524–8531.
[40] H. Tian, Z.e. Yu, A. Hagfeldt, L. Kloo, L. Sun, Organic redox couples and organic counter electrode for efficient organic dye-sensitized solar cells, J. Am. Chem. Soc. 133 (24) (2011) 9413–9422.
[41] R. Hunter, M. Caira, N. Stellenboom, Inexpensive, one-pot synthesis of unsymmetrical disulfides using 1-chlorobenzotriazole, J. Org. Chem. 71 (21) (2006) 8268–8271.
[42] O. Berglund, A. Holmgren, Thioredoxin reductase-mediated hydrogen transfer from Escherichia coli thioredoxin-(SH)2 to phage T4 thioredoxin-S2, J. Biol. Chem. 250 (8) (1975) 2778–2782.
[43] J. Sun, L. Zhang, X. Zhang, Y. Hu, C. Ge, J. Fang, An ultrafast turn-on thiol probe for protein labeling and bioimaging, Analyst 141 (6) (2016) 2009–2015.
[44] Y. Liu, D. Duan, J. Yao, B. Zhang, S. Peng, HuiLong Ma, Y. Song, J. Fang, Dithiaarsanes induce oxidative stress-mediated apoptosis in HL-60 cells by selectively targeting thioredoxin reductase, J. Med. Chem. 57 (12) (2014) 5203–5211.
[45] J. Zhang, Y.A. Li, D. Duan, J. Yao, K. Gao, J. Fang, Inhibition of thioredoxin reductase by alantolactone prompts oxidative stress-mediated apoptosis of HeLa cells, Biochem. Pharmacol. 102 (2016) 34–44.
[46] T. Liu, J. Zhang, X. Han, J. Xu, Y. Wu, J. Fang, Promotion of HeLa cells apoptosis by cynaropicrin involving inhibition of thioredoxin reductase and induction of oxidative stress, Free Radic. Biol. Med. 135 (2019) 216–226.
[47] W. Cai, B. Zhang, D. Duan, J. Wu, J. Fang, Curcumin targeting the thioredoxin system elevates oxidative stress in HeLa cells, Toxicol. Appl. Pharmacol. 262 (3) (2012) 341–348.
[48] B. Kalyanaraman, V. Darley-Usmar, K.J.A. Davies, P.A. Dennery, H.J. Forman, M. B. Grisham, G.E. Mann, K. Moore, L.J. Roberts, H. Ischiropoulos, Measuring reactive oxygen and nitrogen species with fluorescent probes: challenges and limitations, Free Radic. Biol. Med. 52 (1) (2012) 1–6.
[49] S. Gromer, S. Urig, K. Becker, The thioredoxin system–from science to clinic, Med. Res. Rev. 24 (1) (2004) 40–89.
[50] A. Ferino, V. Rapozzi, L.E. Xodo, The ROS-KRAS-Nrf2 axis in the control of the redox homeostasis and the intersection with survival-apoptosis pathways: Implications for photodynamic therapy, J. Photochem. Photobiol. B 202 (2020) 111672, https://doi.org/10.1016/j.jphotobiol.2019.111672.
[51] M.H. Lee, J.H. Han, J.-H. Lee, H.G. Choi, C. Kang, J.S. Kim, Mitochondrial thioredoxin-responding off-on fluorescent probe, J. Am. Chem. Soc. 134 (41) (2012) 17314–17319.
[52] D. Duan, B. Zhang, J. Yao, Y. Liu, J. Fang, Shikonin targets cytosolic thioredoxin reductase to induce ROS-mediated apoptosis in human promyelocytic leukemia HL-60 cells, Free Radic. Biol. Med. 70 (2014) 182–193.
[53] J. Zhang, J. Yao, S. Peng, X. Li, J. Fang, Securinine disturbs redox homeostasis and elicits oxidative stress-mediated apoptosis via targeting thioredoxin reductase, Bba-Mol. Basis Dis. 1863 (1) (2017) 129–138.
[54] J. Zhang, D. Duan, J. Xu, J. Fang, Redox-dependent copper carrier promotes cellular copper uptake and oxidative stress-mediated apoptosis of cancer cells, Acs Appl. Mater. Inter. 10 (39) (2018) 33010–33021.